PCT WORLD INTELLECTUAL PROPERTY ORGANIZATION
International Bureau

INTERNATIONAL APPLICATION PUBLISHED UNDER THE PATENT COOPERATION TREATY (PCT)

(51) International Patent Classification 7 : A61B 5/00 — A1

(11) International Publication Number: WO 00/42912

(43) International Publication Date: 27 July 2000 (27.07.00)

(21) International Application Number: PCT/US00/01967

(22) International Filing Date: 25 January 2000 (25.01.00)

(30) Priority Data:
09/237,153 25 January 1999 (25.01.99) US

(63) Related by Continuation (CON) or Continuation-in-Part (CIP) to Earlier Application
US 09/237,153 (CON)
Filed on 25 January 1999 (25.01.99)

(71) Applicant *(for all designated States except US)*: MASSACHUSETTS INSTITUTE OF TECHNOLOGY [US/US]; 77 Massachusetts Avenue, Cambridge, MA 02139 (US).

(72) Inventors; and

(75) Inventors/Applicants *(for US only)*: BACKMAN, Vadim [US/US]; Apartment 9E1, 550 Memorial Drive, Cambridge, MA 02139 (US). DASARI, Ramanchandra, R. [US/US]; 6 Great Rock Road, Lexington, MA 02421 (US). GURJAR, Rajan [IN/US]; 3/897 Main Street, Cambridge, MA 02139 (US). ITZKAN, Irving [US/US]; 330 Beacon Street, Boston, MA 02116 (US). PERELMAN, Lev [US/US]; 94 Griggs Road #21, Brookline, MA 02146 (US). FELD, Michael, S. [US/US]; 56 Hinckley Road, Newton, MA 02468 (US).

(74) Agents: HOOVER, Thomas, O. et al.; Hamilton, Brook, Smith & Reynolds, P.C., Two Militia Drive, Lexington, MA 02421 (US).

(81) Designated States: AE, AL, AM, AT, AU, AZ, BA, BB, BG, BR, BY, CA, CH, CN, CR, CU, CZ, DE, DK, DM, EE, ES, FI, GB, GD, GE, GH, GM, HR, HU, ID, IL, IN, IS, JP, KE, KG, KP, KR, KZ, LC, LK, LR, LS, LT, LU, LV, MA, MD, MG, MK, MN, MW, MX, NO, NZ, PL, PT, RO, RU, SD, SE, SG, SI, SK, SL, TJ, TM, TR, TT, TZ, UA, UG, US, UZ, VN, YU, ZA, ZW, ARIPO patent (GH, GM, KE, LS, MW, SD, SL, SZ, TZ, UG, ZW), Eurasian patent (AM, AZ, BY, KG, KZ, MD, RU, TJ, TM), European patent (AT, BE, CH, CY, DE, DK, ES, FI, FR, GB, GR, IE, IT, LU, MC, NL, PT, SE), OAPI patent (BF, BJ, CF, CG, CI, CM, GA, GN, GW, ML, MR, NE, SN, TD, TG).

Published
With international search report.
Before the expiration of the time limit for amending the claims and to be republished in the event of the receipt of amendments.

(54) Title: POLARIZED LIGHT SCATTERING SPECTROSCOPY OF TISSUE

(57) Abstract

The present invention relates to the use of polarized light to measure properties of tissue. More particularly, polarized light can be used to detect dysplasia in tissue as the polarization of backscattered light from such tissues is preserved while the contribution of diffusely scattered light from underlying tissues can be removed. A fiber optic system for delivery and collection of light can be used to measure tissues within the human body.

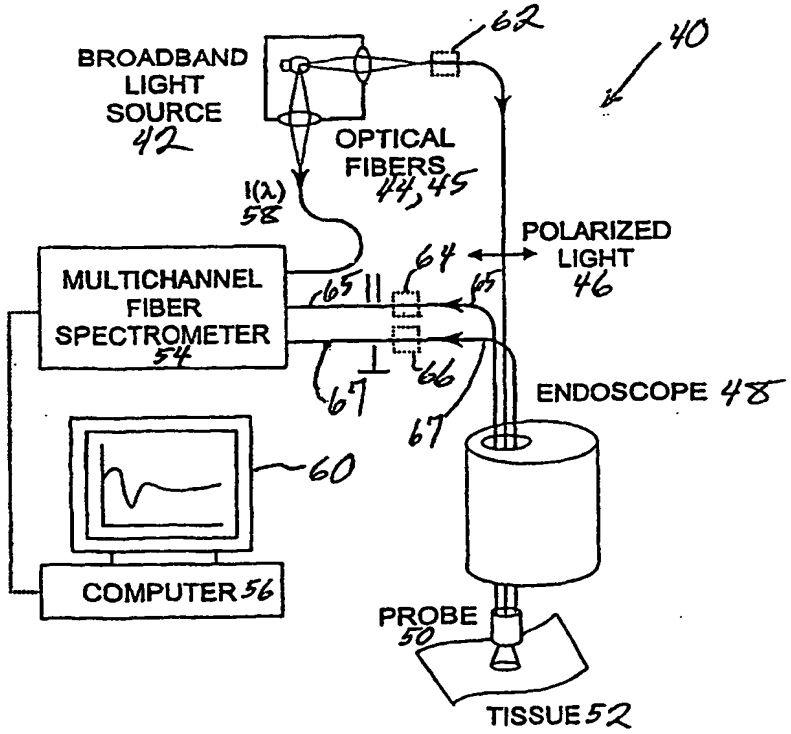

FOR THE PURPOSES OF INFORMATION ONLY

Codes used to identify States party to the PCT on the front pages of pamphlets publishing international applications under the PCT.

AL	Albania	ES	Spain	LS	Lesotho	SI	Slovenia
AM	Armenia	FI	Finland	LT	Lithuania	SK	Slovakia
AT	Austria	FR	France	LU	Luxembourg	SN	Senegal
AU	Australia	GA	Gabon	LV	Latvia	SZ	Swaziland
AZ	Azerbaijan	GB	United Kingdom	MC	Monaco	TD	Chad
BA	Bosnia and Herzegovina	GE	Georgia	MD	Republic of Moldova	TG	Togo
BB	Barbados	GH	Ghana	MG	Madagascar	TJ	Tajikistan
BE	Belgium	GN	Guinea	MK	The former Yugoslav Republic of Macedonia	TM	Turkmenistan
BF	Burkina Faso	GR	Greece			TR	Turkey
BG	Bulgaria	HU	Hungary	ML	Mali	TT	Trinidad and Tobago
BJ	Benin	IE	Ireland	MN	Mongolia	UA	Ukraine
BR	Brazil	IL	Israel	MR	Mauritania	UG	Uganda
BY	Belarus	IS	Iceland	MW	Malawi	US	United States of America
CA	Canada	IT	Italy	MX	Mexico	UZ	Uzbekistan
CF	Central African Republic	JP	Japan	NE	Niger	VN	Viet Nam
CG	Congo	KE	Kenya	NL	Netherlands	YU	Yugoslavia
CH	Switzerland	KG	Kyrgyzstan	NO	Norway	ZW	Zimbabwe
CI	Côte d'Ivoire	KP	Democratic People's Republic of Korea	NZ	New Zealand		
CM	Cameroon			PL	Poland		
CN	China	KR	Republic of Korea	PT	Portugal		
CU	Cuba	KZ	Kazakstan	RO	Romania		
CZ	Czech Republic	LC	Saint Lucia	RU	Russian Federation		
DE	Germany	LI	Liechtenstein	SD	Sudan		
DK	Denmark	LK	Sri Lanka	SE	Sweden		
EE	Estonia	LR	Liberia	SG	Singapore		

POLARIZED LIGHT SCATTERING SPECTROSCOPY OF TISSUE

RELATED APPLICATION

This application claims priority to U.S. Application No. 09/237,153, filed on January 25, 1999, the entire contents of which is incorporated herein by reference.

GOVERNMENT SUPPORT

The invention was supported, in whole or in part, by a grant number P41RR02954 from National Institute for Health. The Government has certain rights in the invention.

BACKGROUND OF THE INVENTION

More then 90% of cancer lesions are epithelial in origin. Several of the most common forms of epithelial cancers such as colorectal, esophageal, bladder, cervical and oral cancers have a well defined, detectable pre-cancer stage called dysplasia. Dysplasia is characterized by sequential accumulation of mutations in defined oncogenes and tumor suppresser genes. If detected, the absolute majority of the dysplastic lesions are curable. Clinical efforts to detect and treat this pre-cancerous stage of epithelial cancer have been shown to reduce the mortality rate.

Diagnosis of epithelial dysplasia remains difficult because it typically does not form macroscopic structures such as polyps, and is usually only visible after

cancer has developed. Standard methods of detecting epithelial dysplasia are based on random biopsies and pathologic examination of the stained biopsy material. However, random biopsies have high sampling error. In many cases less than 1% of the epithelial surface at risk for dysplasia can be examined.

All types of epithelial dysplasia have several common characteristics, namely enlargement of epithelial cell nuclei with an increase in the nuclear to cytoplasmic ratio, nuclear hyperchromatism, and increased number and stratification of epithelial cells. Despite these well-characterized epithelial changes, classification has been difficult as demonstrated by high inter-observer disagreement, even among experienced pathologists.

SUMMARY OF THE INVENTION

Non-invasive, *in-vivo* methods of detecting epithelial dysplasia provide for surveillance of epithelial surfaces, and the pathological diagnosis of pre-cancerous conditions in humans.

Optical techniques are well suited to be a substitution for random biopsies, since they are non-invasive, do not require tissue removal, and can be performed *in-vivo*. Moreover, they are fast (can be applied in real time), are relatively non-expensive, are able to work on microscopic scale, and thus can find very small dysplastic sites. The latter are highly likely to be missed by random biopsies.

The present invention relates to light scattering spectroscopy of polarized light to provide information about scatterers in surface layers of turbid media such as tissue. This process need not utilize fluorescence or absorption spectral features, but rather scattering properties of surface tissues such as epithelial layers. It can characterize properties of large scatterers (cell nuclei) in human epithelium and provide histological information about human tissues and diagnose dysplasia in real time in human organs *in-vivo*.

The idea of light scattering spectroscopy of unpolarized light to determine features of epithelial tissue has been described in U.S. Serial No. 08/948,734 filed on October 10, 1997, and in International Application No. PCT/US98/21450 filed on

October 9, 1998, which designated the United States, the entire contents of these applications being incorporated herein by reference. The major centers of light scattering in epithelium are cellular organelles such as mitochondria and nuclei with the refractive index higher than that of the surrounding cytoplasm. Light backscattered from surface epithelial cell nuclei has an oscillatory wavelength dependent component. The periodicity of this component increases with nuclear size, and its amplitude is related to the density of the nuclei. Thus, by analyzing the amplitude and frequency of the oscillatory component, the density and size distribution of epithelial nuclei can be determined. Normal nuclei have a characteristic diameter l=4-7 μm. In contrast, dysplastic nuclei can be as large as 20 μm. Nuclear size and density are important indicators of neoplastic precancerous changes in biological tissue. The ability to measure nuclear size distribution *in vivo* and in real time has valuable applications in clinical medicine. This enables the diagnosis of precancerous changes in various human organs such as esophagus, colon, bladder, oral cavity, cervix, etc. non-invasively and in-real-time.

Epithelium covers surfaces of organs in the human body. The thickness of epithelium ranges from 20 μm (one cell layer) to a few hundred microns (multiple cell layers). Beneath epithelium there are layers of relatively acellular connective and muscular tissues. Since dysplasia is limited to the epithelium, it is important to differentiate between the signal associated with the epithelium and underlying tissues. The backscattered component which carries information about surface epithelial nuclei is present in light reflected from mucosal tissues. However, it is ordinarily very small in amplitude, and easily masked by a background signal formed by diffuse scattering from the underlying tissue. To analyze that component the background signal must be removed. One can remove the diffuse background by modeling the general spectral features of the background. However, to make the approach more useful in practical medicine, and to be able to diagnose dysplasia *in vivo*, in real time, and in different organs, it is necessary to develop more robust method of removing or significantly reducing the diffuse component of the scattered light.

The present invention provides a method of measuring scattering features of epithelial cells by using polarized light spectroscopy. Note that initially polarized light loses its polarization while traveling through a turbid medium (tissue is an example of turbid medium). On the other hand the light scattered backward after a single scattering preserves polarization. Thus, by removing the nonpolarized component of the scattered light, one is able to distinguish light scattered by epithelial cells. The residual spectrum can be further analyzed so that the size distribution of the nuclei and their density can be determined.

A preferred embodiment of the inventions includes a fiber optic light delivery and collection system for diagnoses of tissue. The fiber optic system can be housed in a probe housing proximal and distal ends where the distal end can be inserted into the various lumens of the human body for in vivo measurements of tissue. Polarizers can be used on the distal ends of both delivery and collection fibers. With optical fibers that preserve the polarization of light, the polarizers can be positioned at the proximal end of the probe. In a three fiber system, the probe can use a central delivery fiber and two off-center collection fibers that collect two different polarization components of light returning from the tissue. The polarizers can be birefringent crystalline materials such as quartz, sapphire or calcite. The calcite must be sealed from the working environment.

BRIEF DESCRIPTION OF THE DRAWINGS

Figure 1 illustrates a preferred embodiment of a polarization-based light scattering spectroscopic system.

Figures 2 A and B are reflectance spectra of the two-layered tissue phantom (polystyrene beads on top of gel containing blood and $BaSO_4$) for parallel and perpendicular polarizations (notice characteristic hemoglobin dips) respectively.

Figures 3 A-D illustrate differences of two polarizations for (A) 4.56 μm beads in water (relative refractive index $n \approx 1.19$), (B) 9.5 μm beads in water ($n \approx 1.19$), (C) 5.7 μm beads in glycol ($n \approx 1.09$), (D) 8.9 μm beads in glycerol ($n \approx 1.07$) where the signals (dashed lines) are in good agreement with Mie

calculations (solid lines) and the absorption features of hemoglobin are completely removed.

Figure 4 is a spectrum of the polarized (residual) component of back-scattered light: experimental data vs. fit of the Mie calculations for the polarized back-scattering for T84 cancerous colonic cells where best fits provide the following sets of parameters: average size 10.2 μm, standard deviation 1.5 μm, relative refractive index 1.045, and the sizes and standard deviations are in agreement with those measured using light microscopy.

Figure 5 is a spectrum of the polarized (residual) component of back-scattered light: experimental data vs. fit of the Mie calculations for the polarized back-scattering for normal intestinal cells where best fits provide the following sets of parameters: average size 5.0 μm, standard deviation 0.5 μm, relative refractive index 1.035, and the sizes and standard deviations are in agreement with those measured using light microscopy.

Figure 6 shows the nuclear size distribution for normal intestinal cells and T84 cancerous colonic cells where in each case, the solid line is the distribution extracted from the data, and the dashed line is the distribution measured using light microscopy.

Figure 7 schematically illustrates a fiber optic probe system for performing in vivo optical measurements of tissue in accordance with the invention.

Figures 8A and 8B show the distal end of a probe of a preferred embodiment of the invention.

Figures 9A-9C illustrate another preferred embodiment of a fiber optic probe in accordance with the invention.

The foregoing and other objects, features and advantages of the invention will be apparent from the following more particular description of preferred embodiments of the invention, as illustrated in the accompanying drawings in which like reference characters refer to the same parts throughout the different views. The drawings are not necessarily to scale, with emphasis being placed upon illustrating the principles of the invention.

DETAILED DESCRIPTION OF THE INVENTION

To determine properties of epithelial cells, one can correlate measured spectrum of the backscattered light with a model or representation. Using Mie theory, which provides the exact solution for the problem of light scattering by spherical objects of arbitrary sizes, the sizes and relative refractive indexes of the scatterers can be determined.

For polarized incident light, light scattered by a spherical particle with diameter d has components which are polarized parallel and perpendicular to the plane of scattering. For a plane polarized wave incident in direction $\hat{s}_0$, light scattered into direction $\hat{s}$ will have components which are polarized parallel (p) and perpendicular (s) to the plane of scattering. Intensities I_p and I_s of these components are related to the intensities of the incident light $I_p^{(0)}$ and $I_s^{(0)}$ as follows:

$$I_p(\hat{s}) = 4\frac{|S_2(\hat{s},\hat{s}_0)|^2}{K^2 d^2} I_p^o(\hat{s}_0) \qquad (1)$$

$$I_s(\hat{s}) = 4\frac{|S_2(\hat{s},\hat{s}_0)|^2}{K^2 d^2} I_p^o(\hat{s}_0) \qquad (2)$$

where k is the wavenumber of the incident light, S_1 and S_2 are scattering amplitudes which can be calculated numerically using Mie theory, and s_1 and s_2 are unit vectors defining propagation of the incident and scattered light. Scattering amplitudes are functions of a scattering angle $\vartheta = \cos^{-1}(s \cdot s_0)$ and are normalized so that integral $\int_0^{\pi} \left(|S_1(\vartheta)|^2 + |S_2(\vartheta)|^2\right) \sin\vartheta d\vartheta$ equals the total elastic scattering cross section.

Now consider an experiment in which linearly polarized incident light, intensity I_0, is distributed over solid angle $\Delta\Omega_0$ and scattering is collected over solid angle $\Delta\Omega$. The polarization, $\hat{\varepsilon}_0$, of the incident light can be decomposed into a

component $\hat{\varepsilon}_p^o$, in the scattering plane (i.e. the plane formed by $\hat{s}$ and $\hat{s}_0$), and a perpendicular component $\hat{\varepsilon}_s^o$. By means of analyzers, we detect two orthogonal components of the scattered light intensity, $I_{\parallel}$ having polarization $\hat{\varepsilon}_a'$ and $I_{\perp}$ having perpendicular polarization $\hat{\varepsilon}_a''$. The scattered intensity components are then given by

$$I_{\parallel} = \frac{2}{\pi k d^2} \int_{\Delta\Omega} d\hat{s} \int_{\Delta\Omega} d\hat{s}_0 I_0(\hat{s}_0) \left| S_2(\hat{s}_0, \hat{s}) \cos\varphi \cos\varphi_0 + S_1(\hat{s}_0, \hat{s}) \sin\varphi \sin\varphi_0 \right|^2$$

(3)

$$I_{\perp} = \frac{2}{\pi k d^2} \int_{\Delta\Omega} d\hat{s} \int_{\Delta\Omega} d\hat{s}_0 I_0(\hat{s}_0) \left| S_2(\hat{s}_0, \hat{s}) \cos\varphi \sin\varphi_0 - S_1(\hat{s}_0, \hat{s}) \sin\varphi \cos\varphi_0 \right|^2$$

(4)

If the incident light is completely collimated ($\Delta\Omega_0 = 0$), light scattered directly backward will be polarized parallel to the incident light polarization. In this case we can orient one of the analyzers parallel to the incident polarization direction ($\hat{\varepsilon}_0 \approx \hat{\varepsilon}_a'$). If the solid angles of the incident and collected light are sufficiently small and approximately equal, both $I_{\parallel}$ and $I_{\perp}$ will be present. However, the analyzer can still be positioned such that ($\hat{\varepsilon}_0 \approx \hat{\varepsilon}_a'$). Thus, in this case the collected light will still be highly polarized, and $I_{\parallel} >> I_{\perp}$. For this case the expression for the residual intensity, $I_{\parallel} - I_{\perp}$ can be simplified:

$$I_{\parallel} - I_{\perp} \approx \frac{4 I_0}{k d^2} \int_0^{\vartheta_0} \mathrm{Re}\left(S_1^*(\vartheta) S_2(\vartheta) \right) \sin\vartheta d\vartheta ,$$

(5)

with $\vartheta_0 = \sqrt{\frac{\Delta\Omega}{2\pi}}$.

Consider a system of two layers of scattering media such as epithelial tissue in which a thin layer of large scattered ($d>>\lambda$) covers a highly turbid layer of underlying tissue. Each of these layers gives rise to a different type of scattering. This two layer system represents optical properties of many human tissues with the first layer correlated with epithelium and second layer correlated with other tissue layers beneath epithelium. The upper layer is optically thin so that it does not allow multiple scattering. Small portions of incident linearly polarized light is backscattered by the particles in the upper layer. The rest of the signal penetrates to the second layer that is optically thick. Light propagating through the second layer is randomized by means of multiple scattering. This diffusive light, if not absorbed in the second layer, returns to the surface. Thus, emerging light has two contributions: one from light backscattered by the particles of the first layer, I_b, and the other being diffusely reflected from the second layer, I_d. I_b has high degree of linear polarization that is parallel to the polarization of the incident light: $I_{\parallel}^{b}>>I_{\perp}^{b}$. As a result of multiple scatterings in the second layer, diffusely reflected light is depolarized and $I_{\parallel}^{d}=I_{\perp}^{d}$. Therefore, the residual intensity of the emerging light $I_{\parallel}-I_{\perp}\approx I_{\parallel}^{b}-I_{\perp}^{b}$ is dominated by the contribution from the upper layer and is substantially free from both absorption and scattering from the tissue below.

Expressions (3)-(5) relate $I_{\parallel}-I_{\perp}$ to the scattering amplitudes S_1 and S_2. The amplitudes depend on the wavelength of the light being scattered $\lambda=\pi/k$, the scatter's size *d* and the ratio of its refractive index to that of the surrounding medium, relative refractive index *n*. Therefore, the spectrum of the residual intensity varies with the scatterer's size and relative refractive index. Thus, sizes and refractive indexes of the scatterers can be found by fitting the representation of the Mie theory using equations (3)-(5) to the residual intensity spectrum.

A system 10 that measures excised tissue samples *in vitro* is illustrated in Figure 1. This system 10 delivers collimated polarized light on tissue 12 and separates two orthogonal polarizations of back-scattered light. The difference of these two components provides information about light scattered in the epithelial layer only. Since linearly polarized light is depolarized faster than circularly

polarized light while passing through a random medium, linear polarization was used. The system provides light from a broad-band source 14 (250 W tungsten lamp, Model 66181, Oriel Instruments, Inc., Stratford, CT) is collimated and then refocused with a small solid angle onto the sample using a fiber 16, a lens 18 and an aperture 20. A broadband polarizer 22 linearly polarizes the beam, before it is delivered to the surface of a scattering medium through beamsplitter 24. The light beam strikes the surface of the sample with an angle ~15° relative to the normal in order to avoid specular reflectance. The diameter of the beam is 2mm. The reflected light is collected in a narrow cone (~0.015 radian) with apertures 26 and mirror 28 and two polarizations, parallel $I_{\|}$ and orthogonal $I_{\perp}$ to the initial polarization, are separated by a broadband polarizing beam splitter cube 28 which also acts as our analyzer (Melles Griot, Inc.). The output from this analyzer is delivered through lenses 30 and 200μm optical fibers 32, 34 (Ocean Optics, Inc., Dunedin, FL) into two channels of a multichannel spectroscope 36 (quadruple spectroscope, Model SQ200, Ocean Optics, Inc., Dunedin, FL). This enables the spectra of both components to be measured simultaneously in the range from 300 nm to 1200 or optionally in the range from 400 nm to 900 nm.

The beams are not perfectly collinear, and when they pass through the polarizer and analyzer cubes this gives rise to a small amount of distortion. Furthermore, the beamsplitter has different reflectivities for *s* and *p* polarizations. A diffusely reflective white surface was used as standard to correct for wavelength non-uniformity, and to calibrate the signals in the two channels. $I_{\perp}(\lambda)$ and $I_{\|}(\lambda)$ were each normalized to the corresponding background spectra, $I_{\perp}^{B}(\lambda)$ and $I_{\|}^{B}(\lambda)$ were each normalized to the corresponding background spectra, $I_{\|}^{B}(\lambda)$ and $I_{\perp}^{B}(\lambda)$ taken with the white diffusing surface. This removed spectral non-uniformities in the light source. Thus, the experiments actually measured the normalized residual intensity, ΔI:

$$\Delta I = \frac{I_{\parallel}}{I_{\parallel}^{B}} - \frac{I_{\perp}}{I_{\perp}^{B}}$$

(5)

Measurements on simple single- and two-layer systems were conducted to determine operational parameters. The single layer system included polystyrene beads of various sizes ranging from 0.5μm to 10μm (Polyscience, Inc.) embedded in de-ionized water, glycol, or glycerol. The thickness of these layers was varied so that the optical thickness τ ranged from 0.1 to 5 a photon propagating through a medium with τ=1, undergoes one scattering event on average). The beads of large sizes 4-10 μm were used to represent cell nuclei. Since the relative refractive index of the polystyrene beads in water is about 1.2 (absolute refractive index is about n=1.59) and is substantially higher than that of the cell nuclei relative to the cytoplasm which is in the range from 1.03 to 1.1, glycol (n_a=1.45) and glycerol (n_a=1.48) were used instead of water to decrease the relative refractive index of the beads and, therefore, better approximate biological conditions.

In the single layer measurements the component of the backscattered light with the same state of polarization as the incoming light (denoted by $I_{\parallel}$) was almost 100 times larger than the component with the polarization orthogonal to the polarization of the incoming light (denoted by $I_{\perp}$). This establishes that single scattering from large spheroidal particles preserves polarization.

In the measurements with two layer models the first layer consisted of polystyrene beads embedded in water, glycol, or glycerol and was prepared as in the single layer measurements. The second layer included a gel containing solution of $BaSO_4$ powder which provided scattering properties of the second layer and human blood. Hemoglobin content of the blood provided absorptive properties to the model. This physical model simulated epithelium and underlying tissues. Adjusting concentrations of the $BaSO_4$ powder and blood, the scattering and absorption properties, can be made similar to those of a biological tissue, since in the optical spectral region hemoglobin is known to be the major absorber.

Figures 2A and 2B shows spectra of the parallel $I_{\parallel}$ and orthogonal $I_{\perp}$ polarized components of the light reflected from a two layer system. In this measurement, the first layer contained beads embedded in glycol. The beads had an average diameter of 4.56 μm. Standard deviation of their sizes was 0.03 μm. Optical thickness of the first layer was $\tau \sim 0.8$. The second layer was optically thick and its scattering and absorptive properties were comparable to those of a biological tissue. The spectrum of $I_{\perp}$ is dominated by characteristic hemoglobin absorption bands. At the same time, characteristic spectral features of light scattered by 4.56 μm beads in the first layer, namely apparent ripple structure, and hemoglobin absorption in the second layer are seen in the spectrum of $I_{\parallel}$.

The residual spectrum ΔI is shown in Figure 3A. No hemoglobin absorption features are seen and the diffusive background coming from the second layer was completely removed. The ripple structure characteristic of scattering from spheres is evident. The comparison with Mie theory representation for scatterers with d = 4.56 μm , Δd=0.03μm and n=1.035 correspond with the μm shown in Figure 3B shows high degree of accuracy. The residual spectra obtained in measurements with other bead sizes (5.7μm, 8.9μm, and 9.5μm) embedded in any of the media used (water, glycol, and glycerol) had no measurable diffusive background component and agreed with Mie theory. Figure 3B shows the agreement between the theory and the measurements for 9.5 μm beads.

Similarly, the results of the measurements for 5.7 μm and 8.9 μm beads in glycerol and glycol are shown in Figures 3(C) and (D) respectively. Mie theory corresponds with the measured values in these cases as well. The high frequency ripple structure decreases as the relative refractive index gets smaller. The law frequency oscillations remain evident. Measurements showed that the instrument was able to detect signal from the bead solution of as low optical thickness as 0.05. Small disagreements seen in the spectrum can result from imperfect calibration of the instrument for the wavelength dependence of the optical elements used. The beams are not perfectly collinear and so there arises some imperfections in the polarized signals from the two channels when the beam passes through the polarizer

and the analyzer elements. Further, the beam splitter used has different reflectivities for the *s* and the *p* polarized beams. However, using just a white standard, signals in the two channels were corrected for any wavelength non-uniformity and further used for calibration of signals.

Measurements with cell monolayers were conducted and the results are described in connection with Figures 4-6. A layer of gel containing solution of $BaSO_4$ powder and human blood under the monolayers is used to represent underlying tissue. The concentrations of the $BaSO_4$ powder and blood, were adjusted to match optical properties of the biological tissue. Three types of cells were measured: normal intestinal cells, T84 cancer colonic cells and the fibroblasts. The measurements were similar to the measurements with beads. Nuclei of cells, however, had relative refractive indexes smaller then those of beads as well as larger size distributions which substantially eliminate the ripple structure. Fitting of the observed residual spectrum to Mie theory was performed. Three parameters in the fitting procedure were average size of the nuclei, standard deviation in size (a Gaussian size distribution was assumed), and relative refractive index.

For normal intestinal cells, the best fit was obtained using $d=5.0\mu m, \Delta d=0.5\mu m$, and $n=1.045$ (Figure 4). For the fibroblast cells, d-7.0 μm, $\Delta d=1.0$ μm and $n=1.051$ were obtained. For the T84 colon cancer cells the corresponding values were $d=9.8$ μm $\Delta d=1.5$ μm, and $n=1.04$ (Figure 5).

In order to check these results, the distribution of the average size of the cell nuclei was measured using light microscopy. The sizes and their standard deviations were in agreement with the parameters from Mie theory. A histogram showing the size distributions obtained for the normal T84 cells are shown in Figure 6. The accuracy of the average size is estimated to be 0.1 μm, and the accuracy in *n* as 0.001. Note the larger value of n obtained for cancerous cells, which is in agreement with the hyperchromaticity of cancer cell nuclei observed in conventional histopathology of stained tissue sections.

The backscattered signal can be described by Mie theory if the average size of the nuclei d, standard deviation in sizes Δd, and relative refractive index n are

varied. Note that in Mie theory, dependence on d and n does not always come as a $(n-1)d$ product. Thus, the residual spectra have enough information to extract d and n simultaneously.

The size distributions for monolayers were compared to light microscopy and were in a good agreement for all three lines of cells. The accuracy of size and standard deviation extraction was approximately 0.1 μm which makes the method useful in differentiating nuclei of different cell types, including cancerous and non-cancerous cells of the same organ.

Ability to detect cell nuclear enlargement and changes in refractive index of the nucleus (which can be related to the amount of DNA and protein in the nucleus) has valuable applications in clinical medicine.

The method of tissue diagnosis can be implemented either in a diagnostic device in which light can be delivered to points on the surface of the tissue, and collected and analyzed at each of those points on the surface of the tissue, and collected and analyzed at each of those points. In an *in vivo* system optical fibers are used to deliver and collect light. The fiber probe can be inserted in the endoscope biopsy channel or any similar device (depending on the type of the procedure and organ under study). Polarizer and analyzer can be placed at the tip of the probe in front of the delivery and collection fibers. Such an instrument can be used during routine endoscopic procedures to detect precancerous changes *in-vivo* in real time.

Such a probe system 40 is shown generally in Figure 7. This system 40 includes a broadband light source 42 that is optically coupled to a delivery fiber 44 extending through probe 50. As schematically shown in Figure 7, the probe 50 can be inserted through a channel in an endoscope 48, however the probe 50 can be constructed to be used separately. In a preferred embodiment described hereinafter, the light from source is directed through a polarizer at the distal end of probe 50. However, in another embodiment using polarization preserving optical fibers, a polarizer 26 can be used at the proximal end of probe fiber 44 to direct polarized light 46 through the fiber. Similarly, the proximal ends of collection fibers 65, 66 can employ polarizing elements 65, 66 respectively to transmit selected polarization

components into the multichannel fiber spectrometer 54. The data can then be processed by computer 56, stored in computer 56, stored in computer memory and displayed on display 60 as needed.

The probe system can include a fiber optic probe having a distal end incorporating polarizers as seen in Figure 8A and 8B.

Figures 8A and 8B show the distal end of a probe 100 for the use of polarized light for in vivo diagnosis. Figure 8A shows a fiber optic device that is divided into three sections, the inner delivery fiber and two sets of collection fibers 150 and 152 that collect different polarization components. The cross-section of Figure 8B shows fibers 156 delivering light onto the tissue 140. They have to pass through a polarizer 120 which is also seen in the cross-section view of Figure 8B. The polarizing element is divided into at least two parts or elements 122, 126. Optical fibers 152 are arranged to collect the back reflected light from the tissue surface.

The backscattered light has two polarization components, corresponding to the parallel and the perpendicular components to the incident light. The two are differentiated by two different birefringent analyzers shown by two sectioned ring elements 122, 126. A first element 122 allows the parallel component to pass through while the second element 126 allows perpendicular component. A portion of element 122 polarizes light exiting fiber 156. As the fibers have low numerical apertures to collect light over very small angles, it is necessary to extend the distance 136 between the fiber ends and the aperture surface 142 opening to the tissue surface 140. It can be as long as 5mm. To avoid spurious internal reflections a glass block 130 is shown having refractive index n_2 lower than that of the shield 132 with refractive index n_1. The shield 132 can be coated with an absorbing element so that light hitting the boundaries is refracted out and then absorbed by the absorbing coating on the outer wall of the shield 132. The glass element 130 is beveled to avoid specular reflections from the tissue surface as it is described to increase the relative signal strength of the back-scattering. The light having the two orthogonal

polarizations is separated and coupled to two spectrometer channels for detection and analysis.

Another preferred embodiment of a fiber optic probe 160 is illustrated in Figures 9A-9C. In this embodiment, delivery 156 and collection 162 fibers are housed in flexible tube 164 that is attached to a distal annular housing 166. Housing 166 includes a fiber retainer 106 and a polarizer 168 which can be a birefringent crystal such as calcite, quartz or sapphire. Delivery fiber 156 delivers light from source 42 to polarizer 168 which delivers ordinary ray 170 through aperture 175 and window 178. Light returning through aperture 175 has ordinary 170 and extraordinary 172 components. The perpendicular component is collected by fibers 162 and the parallel component is collected by fibers 161. The delivery fiber 156 is positioned along the optical axis 176 of the crystal 168. Fibers 161, 156 are aligned along the aperture 175 of absorbing plate 178.

While this invention has been particularly shown and described with references to preferred embodiments thereof, it will be understood by those skilled in the art that various changes in form and details may be made therein without departing from the spirit and scope of the invention as defined by the appended claims.

CLAIMS

What is claimed is:

1. A method of analyzing polarized light comprising:

detecting polarized light returning from a region of interest; and

determining a characteristic of the region of interest by analyzing the detected polarized light.

2. The method of Claim 1 further comprising determining a size of tissue cells within the region of interest.

3. The method of Claim 1 further comprising removing a nonpolarized component of the light returning from tissue.

4. The method of Claim 1 further comprising providing a fiber optic probe and collecting polarized light from the tissue with the probe.

5. The method of Claim 1 further comprising detecting the polarized backscattered light and forming a spectrum with the detected light, the spectrum including wavelengths in the range of 300 nm to 1200 nm.

6. The method of Claim 1 further comprising determining a fracture index of the region of interest with the detected polarized light

7. The method of Claim 1 further comprising detecting light from a tissue sample.

8. The method of Claim 7 further comprising providing a broadband light source and a filter wheel and delivering polarized light onto the tissue sample.

9. The method of Claim 1 further comprising separating polarization components of light returning from the region of interest and analyzing the two components to remove non-polarized backscattered light from the detected light.

10. A fiber optic probe for measuring a layer of tissue comprising:

a fiber optic cable optically coupled to a light source, the fiber optic cable delivering polarized light onto the tissue; and

a detector system that detects the polarization components of light received from the tissue.

11. The probe of Claim 10 further comprising a polarizer that polarizes light from the light source, the polarizer positioned at a distal end of the fiber optic cable.

12. The probe of Claim 10 further comprising an analyzer that separates polarization components returning from tissue through the fiber optic cable.

13. The probe of Claim 10 further comprising an endoscope having a channel through which the probe is inserted.

14. The probe of Claim 12 wherein the analyzer comprises a polarizing beam splitter.

15. The probe of Claim 12 wherein the analyzer is positioned at a distal end of the fiber optic cable.

16. The probe of Claim 10 further comprising a plurality of polarization filters at the distal end of the probe.

17. The probe of Claim 10 wherein the light source comprises a broadband light source and a filter wheel.

18. The probe of Claim 10 further comprising a spectrometer optically coupled to the fiber optic probe.

19. The probe of Claim 10 further comprising an electronic memory that stores spectra, the spectra including wavelengths in the range of 300nm to 1200nm.

20. The probe of Claim 10 further comprising a computer that analyzes detected spectra to determine whether a surface layer of tissue is normal or epithelial dysplasia.

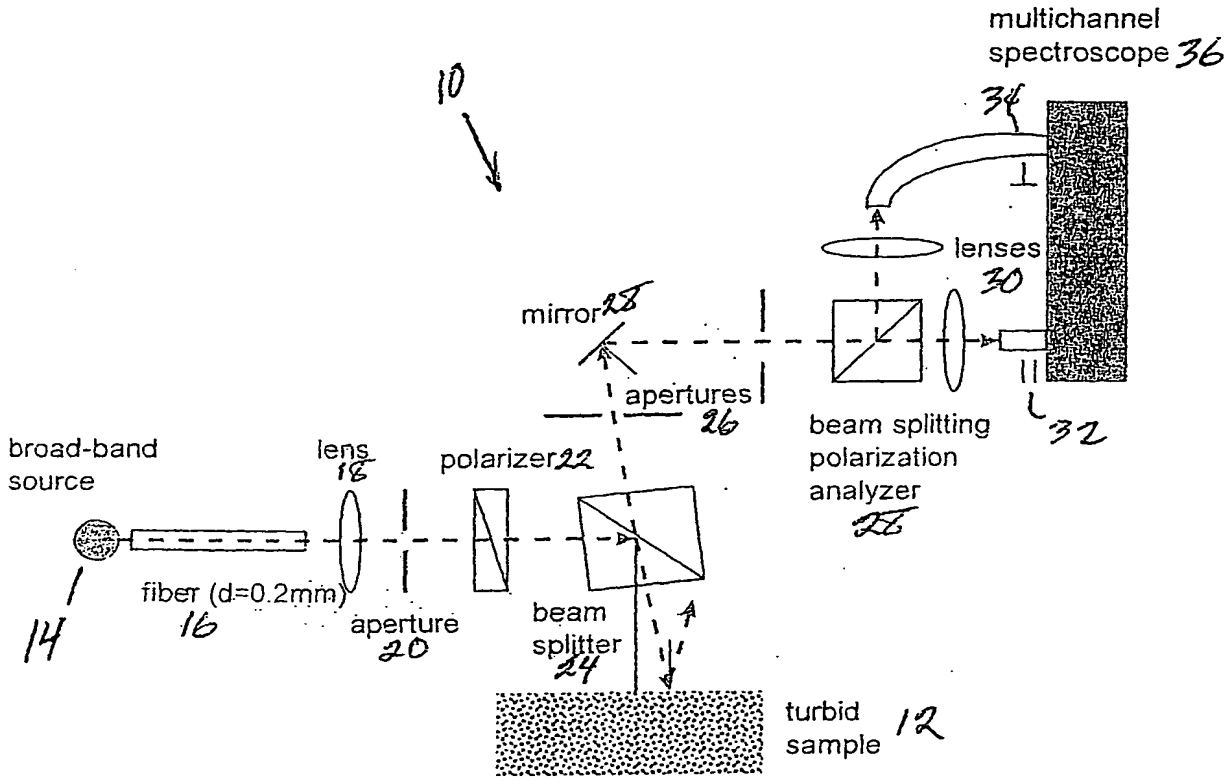

Figure 1

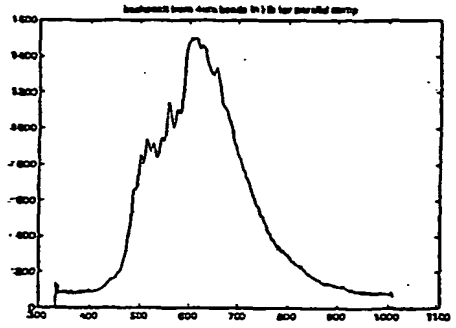

Figure 2A

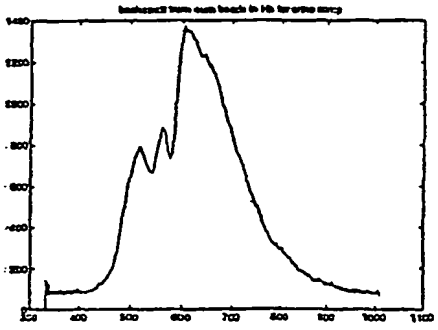

Figure 2B

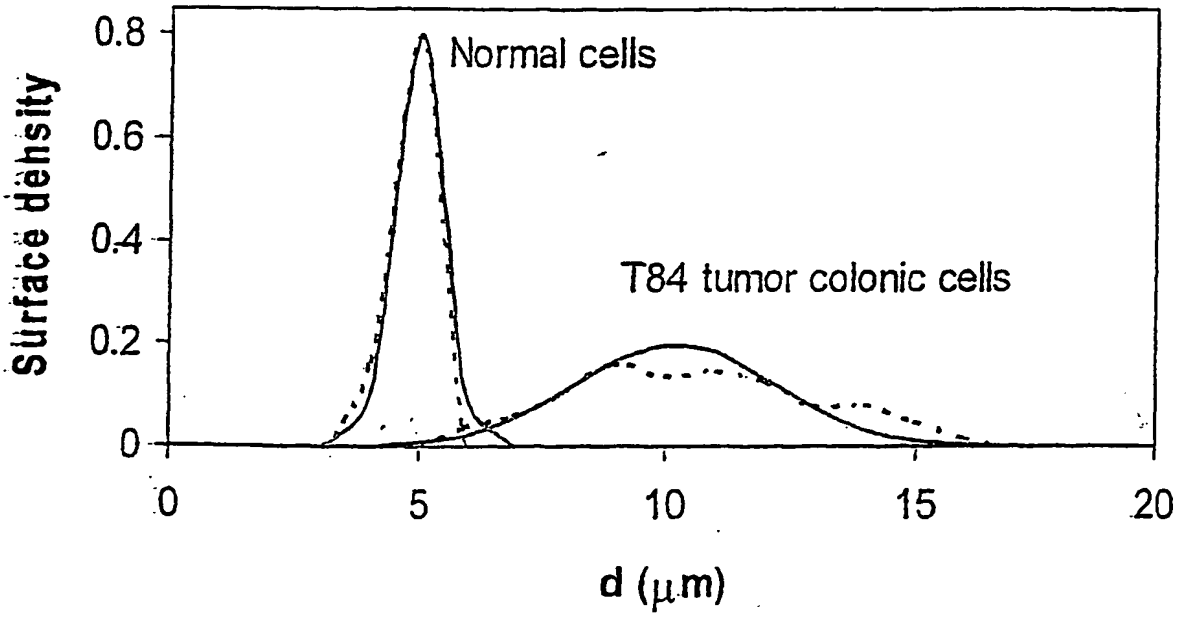

Figure 5

Figure 3A

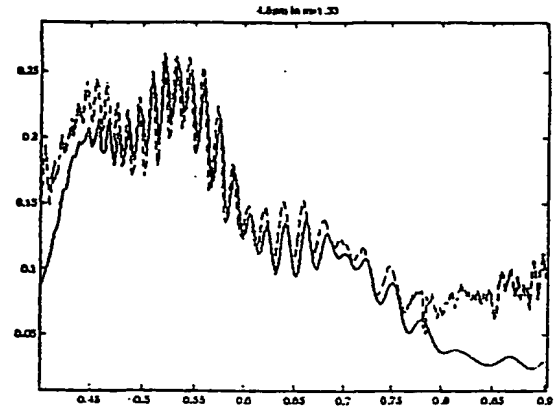

Figure 3B

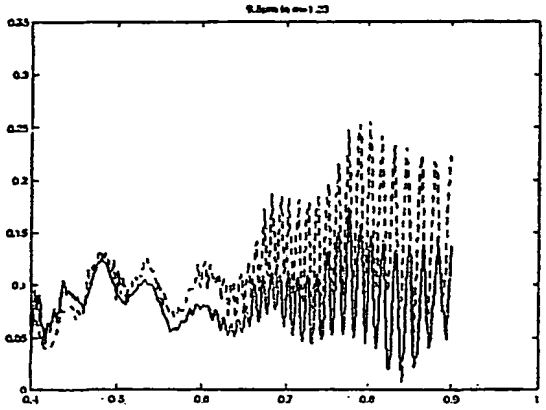

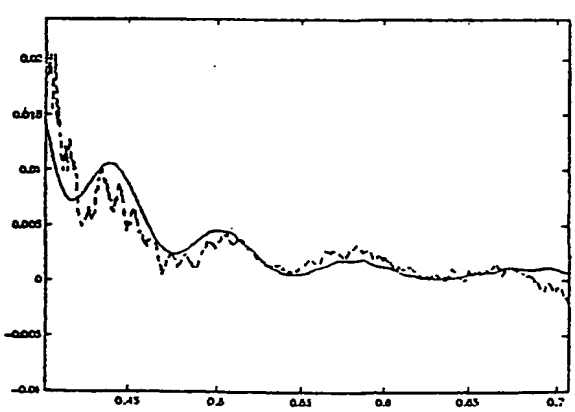

Figure 3C

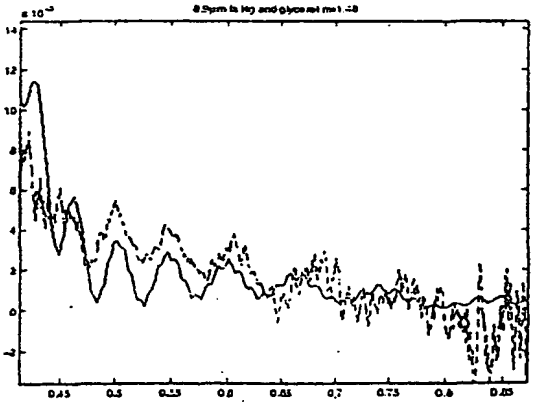

Figure 3D

Figure 4

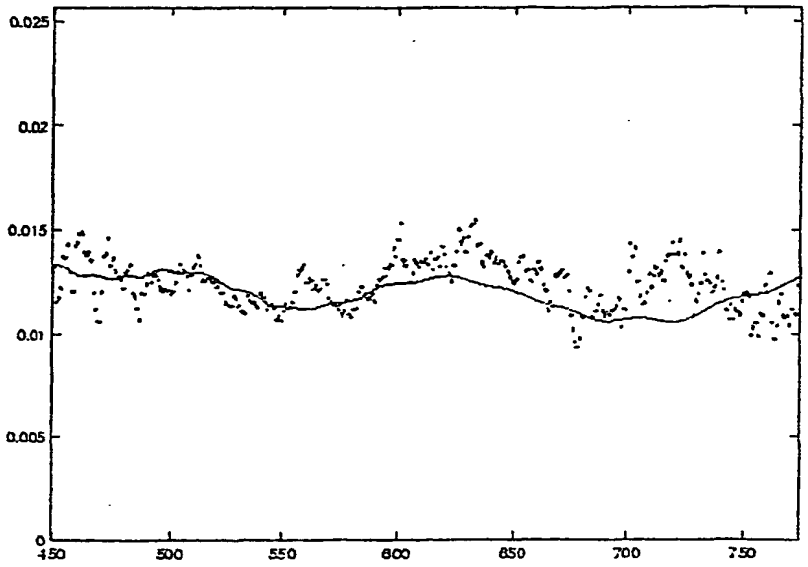

Figure 5

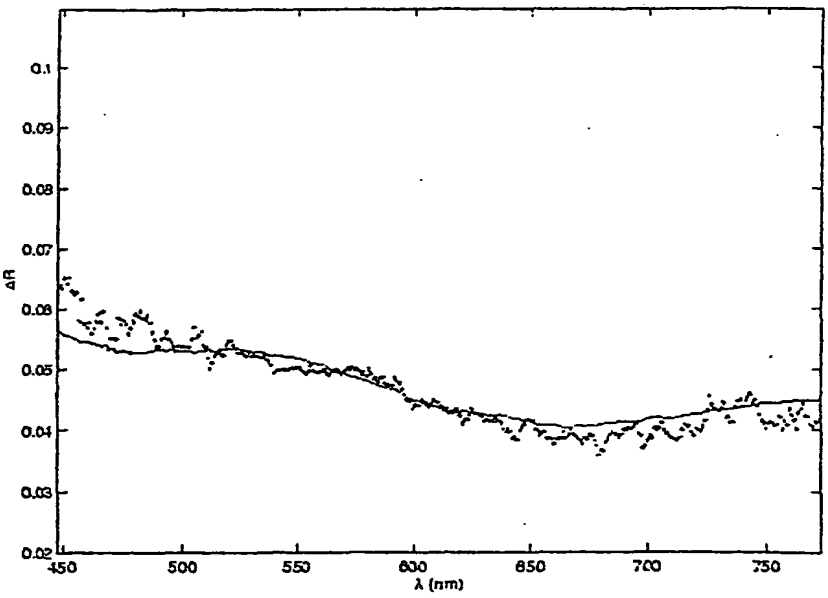

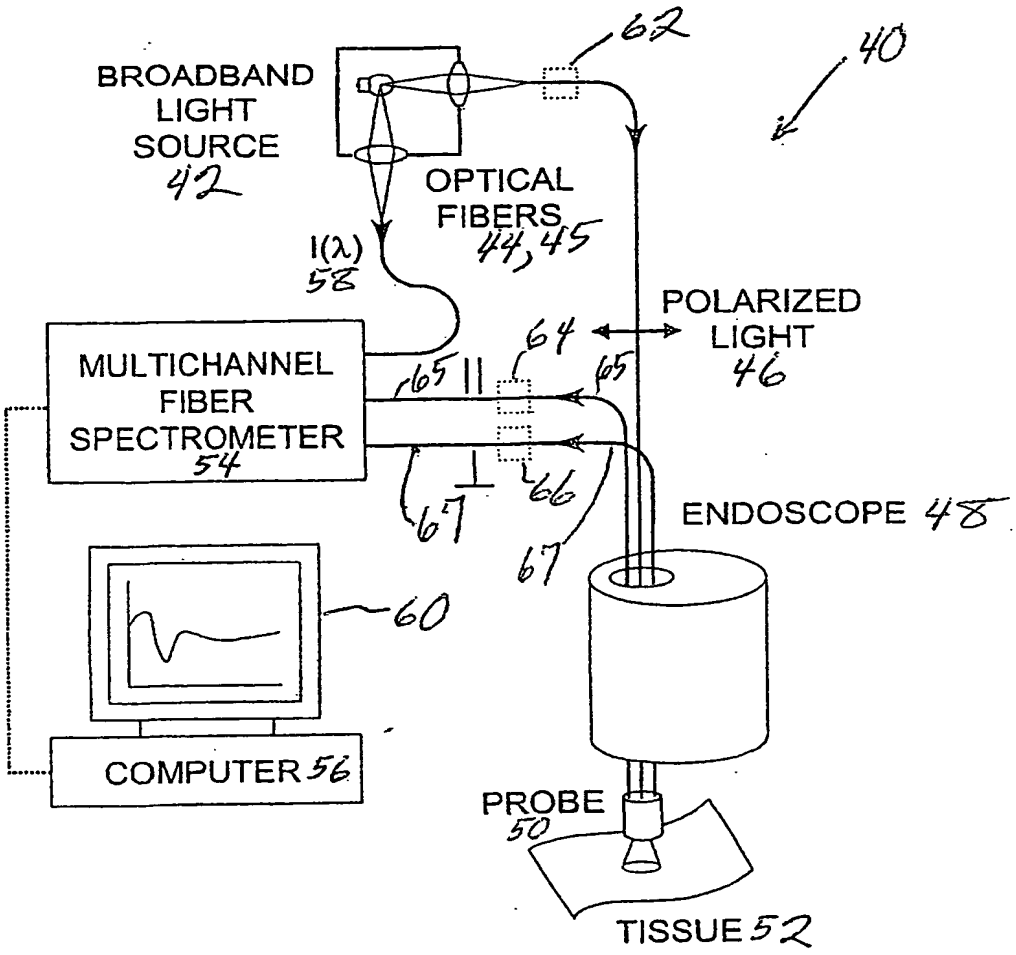
62
40
BROADBAND LIGHT SOURCE 42
OPTICAL FIBERS 44, 45
I(λ) 58
POLARIZED LIGHT 46
64
65
65
MULTICHANNEL FIBER SPECTROMETER 54
67
66
67
ENDOSCOPE 48
60
COMPUTER 56
PROBE 50
TISSUE 52

Figure 7

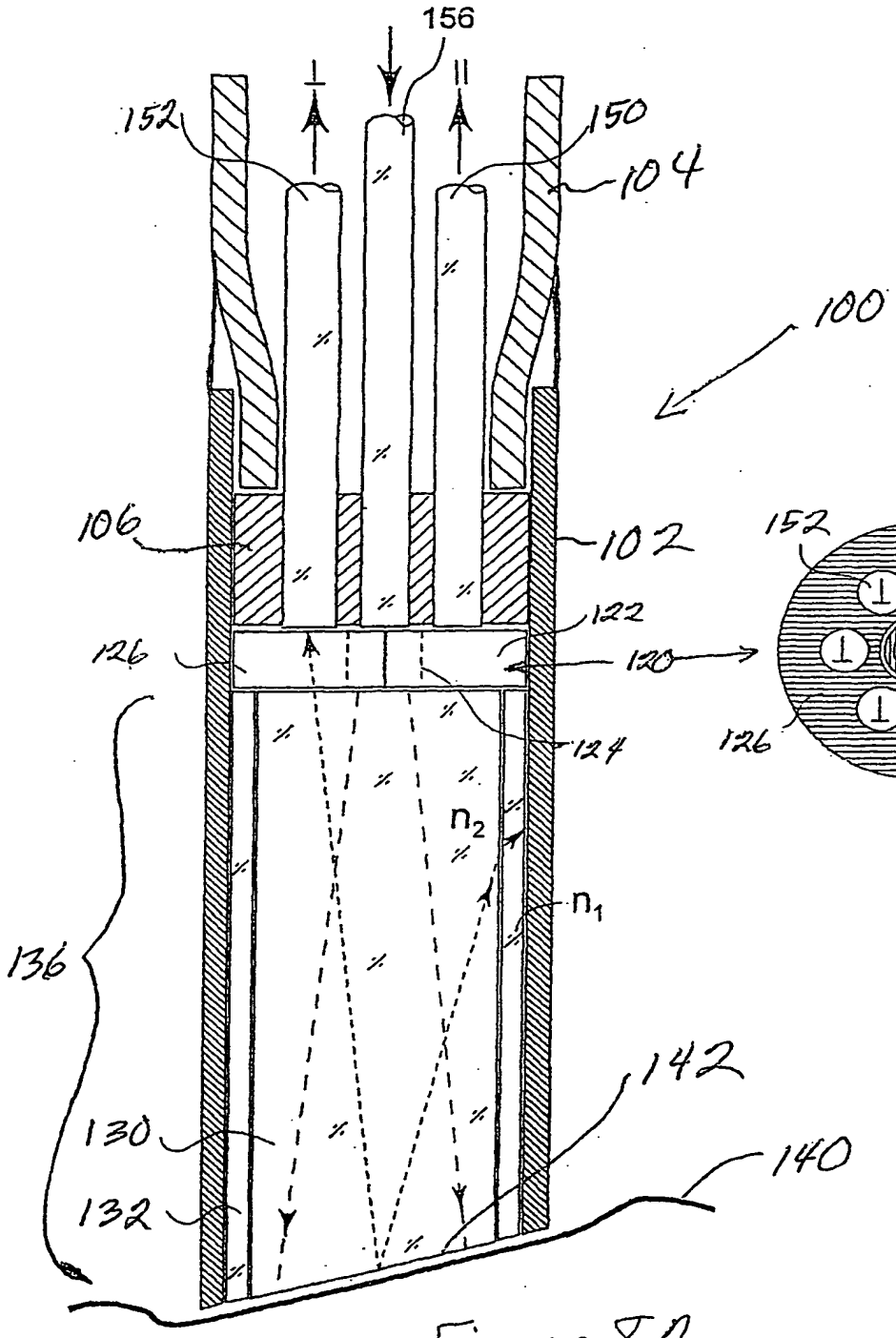

Figure 8A

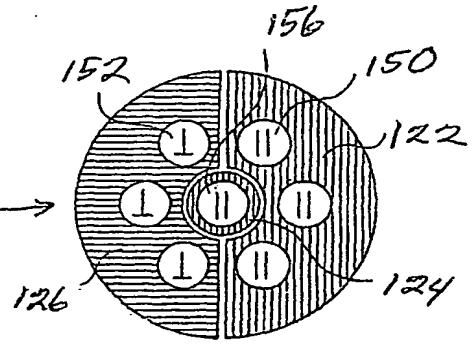

Figure 8B

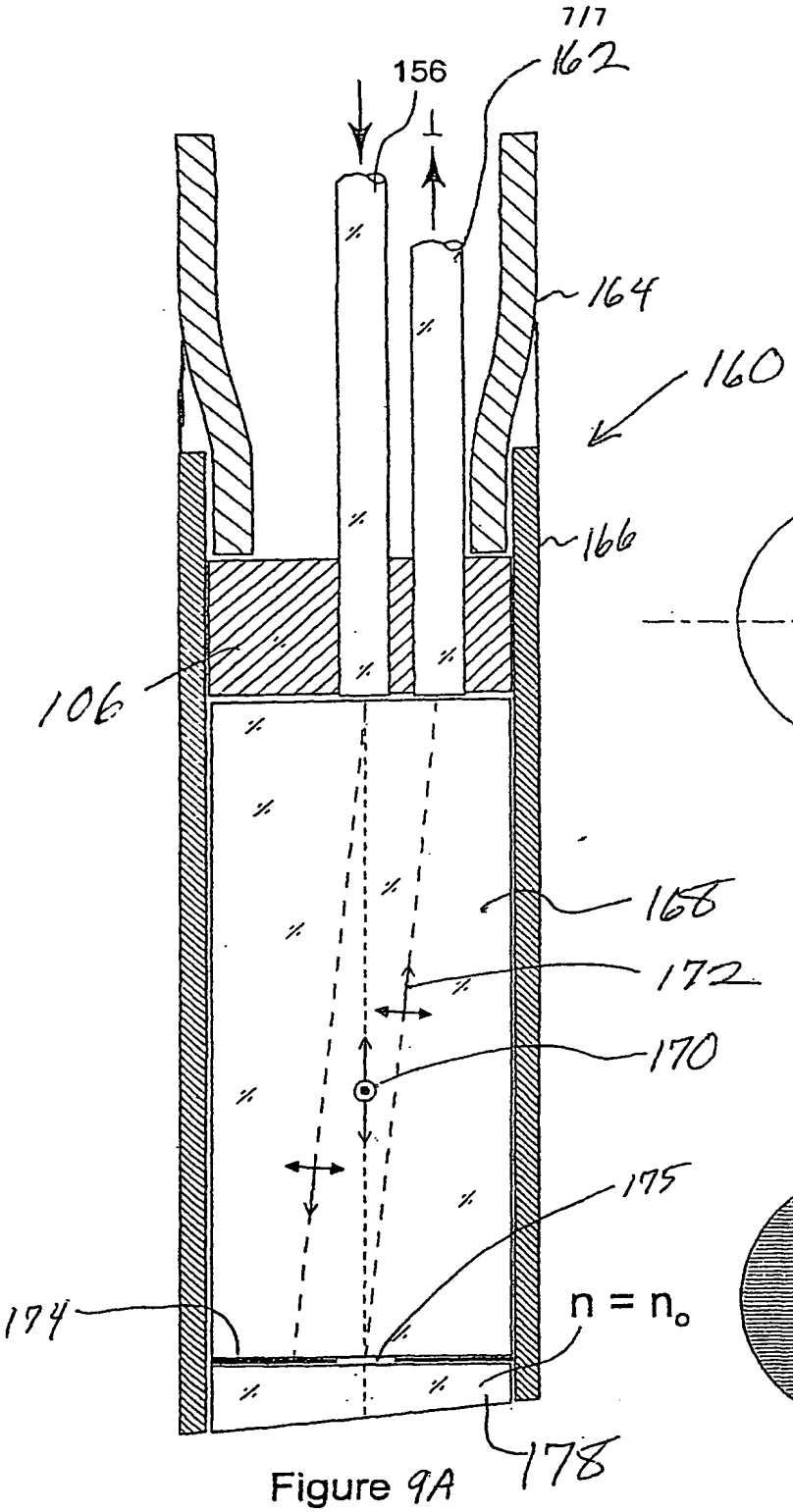

Figure 9A

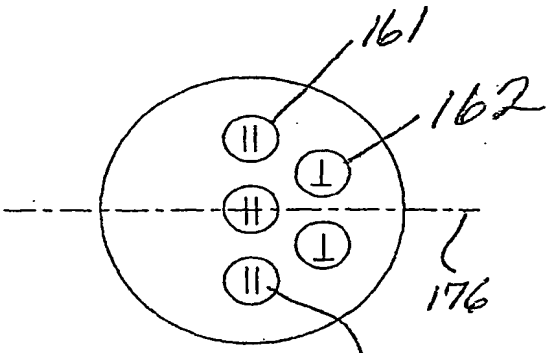

Figure 9B

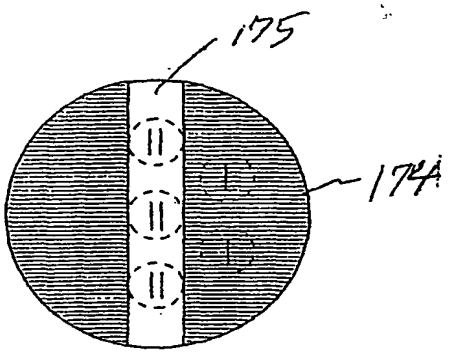

Figure 9C

(12) INTERNATIONAL APPLICATION PUBLISHED UNDER THE PATENT COOPERATION TREATY (PCT)

CORRECTED VERSION

(19) World Intellectual Property Organization
International Bureau

(43) International Publication Date
27 July 2000 (27.07.2000)

PCT

(10) International Publication Number
WO 00/42912 A1

(51) International Patent Classification[7]: A61B 5/00

(21) International Application Number: PCT/US00/01967

(22) International Filing Date: 25 January 2000 (25.01.2000)

(25) Filing Language: English

(26) Publication Language: English

(30) Priority Data:
09/237,153 25 January 1999 (25.01.1999) US

(63) Related by continuation (CON) or continuation-in-part (CIP) to earlier application:
US 09/237,153 (CON)
Filed on 25 January 1999 (25.01.1999)

(71) Applicant *(for all designated States except US)*: **MASSACHUSETTS INSTITUTE OF TECHNOLOGY** [US/US]; 77 Massachusetts Avenue, Cambridge, MA 02139 (US).

(72) Inventors; and
(75) Inventors/Applicants *(for US only)*: **BACKMAN, Vadim** [US/US]; Apartment 9E1, 550 Memorial Drive, Cambridge, MA 02139 (US). **DASARI, Ramanchandra, R.** [US/US]; 6 Great Rock Road, Lexington, MA 02421 (US). **GURJAR, Rajan** [IN/US]; 3/897 Main Street, Cambridge, MA 02139 (US). **ITZKAN, Irving** [US/US]; 330 Beacon Street, Boston, MA 02116 (US). **PERELMAN, Lev** [US/US]; 94 Griggs Road #21, Brookline, MA 02146 (US). **FELD, Michael, S.** [US/US]; 56 Hinckley Road, Newton, MA 02468 (US).

[Continued on next page]

(54) Title: POLARIZED LIGHT SCATTERING SPECTROSCOPY OF TISSUE

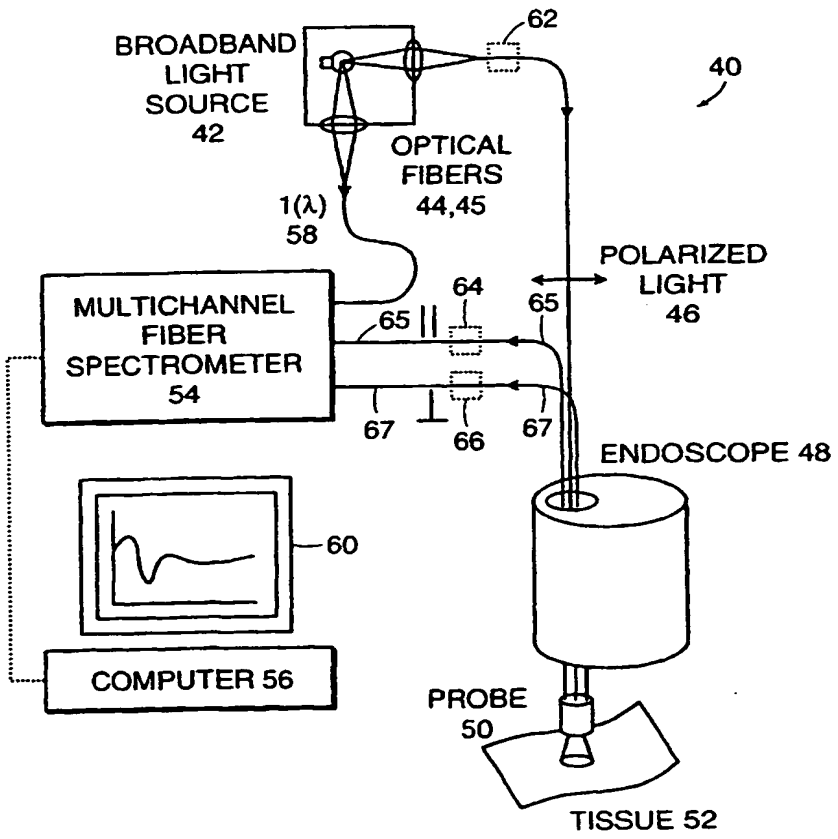

(57) Abstract: The present invention relates to the use of polarized light to measure properties of tissue. More particularly, polarized light can be used to detect dysplasia in tissue as the polarization of backscattered light from such tissues is preserved while the contribution of diffusely scattered light from underlying tissues can be removed. A fiber optic system for delivery and collection of light can be used to measure tissues within the human body.

WO 00/42912 A1

(74) **Agents:** **HOOVER, Thomas, O.** et al.; Hamilton, Brook, Smith & Reynolds, P.C., Two Militia Drive, Lexington, MA 02421 (US).

(81) **Designated States** *(national)*: AE, AL, AM, AT, AU, AZ, BA, BB, BG, BR, BY, CA, CH, CN, CR, CU, CZ, DE, DK, DM, EE, ES, FI, GB, GD, GE, GH, GM, HR, HU, ID, IL, IN, IS, JP, KE, KG, KP, KR, KZ, LC, LK, LR, LS, LT, LU, LV, MA, MD, MG, MK, MN, MW, MX, NO, NZ, PL, PT, RO, RU, SD, SE, SG, SI, SK, SL, TJ, TM, TR, TT, TZ, UA, UG, US, UZ, VN, YU, ZA, ZW.

(84) **Designated States** *(regional)*: ARIPO patent (GH, GM, KE, LS, MW, SD, SL, SZ, TZ, UG, ZW), Eurasian patent (AM, AZ, BY, KG, KZ, MD, RU, TJ, TM), European patent (AT, BE, CH, CY, DE, DK, ES, FI, FR, GB, GR, IE, IT, LU, MC, NL, PT, SE), OAPI patent (BF, BJ, CF, CG, CI, CM, GA, GN, GW, ML, MR, NE, SN, TD, TG).

Published:
— *with international search report*

(48) **Date of publication of this corrected version:**
28 March 2002

(15) **Information about Correction:**
see PCT Gazette No. 13/2002 of 28 March 2002, Section II

For two-letter codes and other abbreviations, refer to the "Guidance Notes on Codes and Abbreviations" appearing at the beginning of each regular issue of the PCT Gazette.

POLARIZED LIGHT SCATTERING SPECTROSCOPY OF TISSUE

RELATED APPLICATION

This application claims priority to U.S. Application No. 09/237,153, filed on January 25, 1999, the entire contents of which is incorporated herein by reference.

GOVERNMENT SUPPORT

The invention was supported, in whole or in part, by a grant number P41RR02954 from National Institute for Health. The Government has certain rights in the invention.

BACKGROUND OF THE INVENTION

More then 90% of cancer lesions are epithelial in origin. Several of the most common forms of epithelial cancers such as colorectal, esophageal, bladder, cervical and oral cancers have a well defined, detectable pre-cancer stage called dysplasia. Dysplasia is characterized by sequential accumulation of mutations in defined oncogenes and tumor suppresser genes. If detected, the absolute majority of the dysplastic lesions are curable. Clinical efforts to detect and treat this pre-cancerous stage of epithelial cancer have been shown to reduce the mortality rate.

Diagnosis of epithelial dysplasia remains difficult because it typically does not form macroscopic structures such as polyps, and is usually only visible after

cancer has developed. Standard methods of detecting epithelial dysplasia are based on random biopsies and pathologic examination of the stained biopsy material. However, random biopsies have high sampling error. In many cases less than 1% of the epithelial surface at risk for dysplasia can be examined.

All types of epithelial dysplasia have several common characteristics, namely enlargement of epithelial cell nuclei with an increase in the nuclear to cytoplasmic ratio, nuclear hyperchromatism, and increased number and stratification of epithelial cells. Despite these well-characterized epithelial changes, classification has been difficult as demonstrated by high inter-observer disagreement, even among experienced pathologists.

SUMMARY OF THE INVENTION

Non-invasive, *in-vivo* methods of detecting epithelial dysplasia provide for surveillance of epithelial surfaces, and the pathological diagnosis of pre-cancerous conditions in humans.

Optical techniques are well suited to be a substitution for random biopsies, since they are non-invasive, do not require tissue removal, and can be performed *in-vivo*. Moreover, they are fast (can be applied in real time), are relatively non-expensive, are able to work on microscopic scale, and thus can find very small dysplastic sites. The latter are highly likely to be missed by random biopsies.

The present invention relates to light scattering spectroscopy of polarized light to provide information about scatterers in surface layers of turbid media such as tissue. This process need not utilize fluorescence or absorption spectral features, but rather scattering properties of surface tissues such as epithelial layers. It can characterize properties of large scatterers (cell nuclei) in human epithelium and provide histological information about human tissues and diagnose dysplasia in real time in human organs *in-vivo*.

The idea of light scattering spectroscopy of unpolarized light to determine features of epithelial tissue has been described in U.S. Serial No. 08/948,734 filed on October 10, 1997, and in International Application No. PCT/US98/21450 filed on

October 9, 1998, which designated the United States, the entire contents of these applications being incorporated herein by reference. The major centers of light scattering in epithelium are cellular organelles such as mitochondria and nuclei with the refractive index higher than that of the surrounding cytoplasm. Light backscattered from surface epithelial cell nuclei has an oscillatory wavelength dependent component. The periodicity of this component increases with nuclear size, and its amplitude is related to the density of the nuclei. Thus, by analyzing the amplitude and frequency of the oscillatory component, the density and size distribution of epithelial nuclei can be determined. Normal nuclei have a characteristic diameter l=4-7 μm. In contrast, dysplastic nuclei can be as large as 20 μm. Nuclear size and density are important indicators of neoplastic precancerous changes in biological tissue. The ability to measure nuclear size distribution *in vivo* and in real time has valuable applications in clinical medicine. This enables the diagnosis of precancerous changes in various human organs such as esophagus, colon, bladder, oral cavity, cervix, etc. non-invasively and in-real-time.

Epithelium covers surfaces of organs in the human body. The thickness of epithelium ranges from 20 μm (one cell layer) to a few hundred microns (multiple cell layers). Beneath epithelium there are layers of relatively acellular connective and muscular tissues. Since dysplasia is limited to the epithelium, it is important to differentiate between the signal associated with the epithelium and underlying tissues. The backscattered component which carries information about surface epithelial nuclei is present in light reflected from mucosal tissues. However, it is ordinarily very small in amplitude, and easily masked by a background signal formed by diffuse scattering from the underlying tissue. To analyze that component the background signal must be removed. One can remove the diffuse background by modeling the general spectral features of the background. However, to make the approach more useful in practical medicine, and to be able to diagnose dysplasia *in vivo*, in real time, and in different organs, it is necessary to develop more robust method of removing or significantly reducing the diffuse component of the scattered light.

The present invention provides a method of measuring scattering features of epithelial cells by using polarized light spectroscopy. Note that initially polarized light loses its polarization while traveling through a turbid medium (tissue is an example of turbid medium). On the other hand the light scattered backward after a single scattering preserves polarization. Thus, by removing the nonpolarized component of the scattered light, one is able to distinguish light scattered by epithelial cells. The residual spectrum can be further analyzed so that the size distribution of the nuclei and their density can be determined.

A preferred embodiment of the inventions includes a fiber optic light delivery and collection system for diagnoses of tissue. The fiber optic system can be housed in a probe housing proximal and distal ends where the distal end can be inserted into the various lumens of the human body for in vivo measurements of tissue. Polarizers can be used on the distal ends of both delivery and collection fibers. With optical fibers that preserve the polarization of light, the polarizers can be positioned at the proximal end of the probe. In a three fiber system, the probe can use a central delivery fiber and two off-center collection fibers that collect two different polarization components of light returning from the tissue. The polarizers can be birefringent crystalline materials such as quartz, sapphire or calcite. The calcite must be sealed from the working environment.

BRIEF DESCRIPTION OF THE DRAWINGS

Figure 1 illustrates a preferred embodiment of a polarization-based light scattering spectroscopic system.

Figures 2 A and B are reflectance spectra of the two-layered tissue phantom (polystyrene beads on top of gel containing blood and $BaSO_4$) for parallel and perpendicular polarizations (notice characteristic hemoglobin dips) respectively.

Figures 3 A-D illustrate differences of two polarizations for (A) 4.56 μm beads in water (relative refractive index $n \approx 1.19$), (B) 9.5 μm beads in water ($n \approx 1.19$), (C) 5.7 μm beads in glycol ($n \approx 1.09$), (D) 8.9 μm beads in glycerol ($n \approx 1.07$) where the signals (dashed lines) are in good agreement with Mie

calculations (solid lines) and the absorption features of hemoglobin are completely removed.

Figure 4 is a spectrum of the polarized (residual) component of back-scattered light: experimental data vs. fit of the Mie calculations for the polarized back-scattering for T84 cancerous colonic cells where best fits provide the following sets of parameters: average size 10.2 μm, standard deviation 1.5 μm, relative refractive index 1.045, and the sizes and standard deviations are in agreement with those measured using light microscopy.

Figure 5 is a spectrum of the polarized (residual) component of back-scattered light: experimental data vs. fit of the Mie calculations for the polarized back-scattering for normal intestinal cells where best fits provide the following sets of parameters: average size 5.0 μm, standard deviation 0.5 μm, relative refractive index 1.035, and the sizes and standard deviations are in agreement with those measured using light microscopy.

Figure 6 shows the nuclear size distribution for normal intestinal cells and T84 cancerous colonic cells where in each case, the solid line is the distribution extracted from the data, and the dashed line is the distribution measured using light microscopy.

Figure 7 schematically illustrates a fiber optic probe system for performing in vivo optical measurements of tissue in accordance with the invention.

Figures 8A and 8B show the distal end of a probe of a preferred embodiment of the invention.

Figures 9A-9C illustrate another preferred embodiment of a fiber optic probe in accordance with the invention.

The foregoing and other objects, features and advantages of the invention will be apparent from the following more particular description of preferred embodiments of the invention, as illustrated in the accompanying drawings in which like reference characters refer to the same parts throughout the different views. The drawings are not necessarily to scale, with emphasis being placed upon illustrating the principles of the invention.

DETAILED DESCRIPTION OF THE INVENTION

To determine properties of epithelial cells, one can correlate measured spectrum of the backscattered light with a model or representation. Using Mie theory, which provides the exact solution for the problem of light scattering by spherical objects of arbitrary sizes, the sizes and relative refractive indexes of the scatterers can be determined.

For polarized incident light, light scattered by a spherical particle with diameter d has components which are polarized parallel and perpendicular to the plane of scattering. For a plane polarized wave incident in direction $\hat{s}_0$, light scattered into direction $\hat{s}$ will have components which are polarized parallel (p) and perpendicular (s) to the plane of scattering. Intensities I_p and I_s of these components are related to the intensities of the incident light $I_p^{(0)}$ and $I_s^{(0)}$ as follows:

$$I_p(\hat{s}) = 4\frac{|S_2(\hat{s},\hat{s}_0)|^2}{K^2d^2} I_p^o(\hat{s}_0) \qquad (1)$$

$$I_s(\hat{s}) = 4\frac{|S_2(\hat{s},\hat{s}_0)|^2}{K^2d^2} I_p^o(\hat{s}_0) \qquad (2)$$

where k is the wavenumber of the incident light, S_1 and S_2 are scattering amplitudes which can be calculated numerically using Mie theory, and s_1 and s_2 are unit vectors defining propagation of the incident and scattered light. Scattering amplitudes are functions of a scattering angle $\vartheta = \cos^{-1}(s \cdot s_0)$ and are normalized so that integral $\int_0^{\pi} \left(|S_1(\vartheta)|^2 + |S_2(\vartheta)|^2\right) \sin\vartheta d\vartheta$ equals the total elastic scattering cross section.

Now consider an experiment in which linearly polarized incident light, intensity I_0, is distributed over solid angle $\Delta\Omega_0$ and scattering is collected over solid angle $\Delta\Omega$. The polarization, $\hat{\varepsilon}_0$, of the incident light can be decomposed into a

component $\hat{\varepsilon}_p^o$, in the scattering plane (i.e. the plane formed by $\hat{s}$ and $\hat{s}_0$), and a perpendicular component $\hat{\varepsilon}_s^o$. By means of analyzers, we detect two orthogonal components of the scattered light intensity, $I_{\parallel}$ having polarization $\hat{\varepsilon}_a'$ and $I_{\perp}$ having perpendicular polarization $\hat{\varepsilon}_a''$. The scattered intensity components are then given by

$$I_{\parallel} = \frac{2}{\pi k d^2} \int_{\Delta\Omega} d\hat{s} \int_{\Delta\Omega} d\hat{s}_0 I_0(\hat{s}_0) \left| S_2(\hat{s}_0, \hat{s}) \cos\varphi \cos\varphi_0 + S_1(\hat{s}_0, \hat{s}) \sin\varphi \sin\varphi_0 \right|^2$$

(3)

$$I_{\perp} = \frac{2}{\pi k d^2} \int_{\Delta\Omega} d\hat{s} \int_{\Delta\Omega} d\hat{s}_0 I_0(\hat{s}_0) \left| S_2(\hat{s}_0, \hat{s}) \cos\varphi \sin\varphi_0 - S_1(\hat{s}_0, \hat{s}) \sin\varphi \cos\varphi_0 \right|^2$$

(4)

If the incident light is completely collimated ($\Delta\Omega_0 = 0$), light scattered directly backward will be polarized parallel to the incident light polarization. In this case we can orient one of the analyzers parallel to the incident polarization direction ($\hat{\varepsilon}_0 \approx \hat{\varepsilon}_a'$). If the solid angles of the incident and collected light are sufficiently small and approximately equal, both $I_{\parallel}$ and $I_{\perp}$ will be present. However, the analyzer can still be positioned such that ($\hat{\varepsilon}_0 \approx \hat{\varepsilon}_a'$). Thus, in this case the collected light will still be highly polarized, and $I_{\parallel} >> I_{\perp}$. For this case the expression for the residual intensity, $I_{\parallel} - I_{\perp}$ can be simplified:

$$I_{\parallel} - I_{\perp} \approx \frac{4 I_0}{k d^2} \int_0^{\vartheta_0} \mathrm{Re}\left(S_1^*(\vartheta) S_2(\vartheta) \right) \sin\vartheta d\vartheta ,$$

(5)

with $\vartheta_0 = \sqrt{\frac{\Delta\Omega}{2\pi}}$.

Consider a system of two layers of scattering media such as epithelial tissue in which a thin layer of large scattered ($d>>\lambda$) covers a highly turbid layer of underlying tissue. Each of these layers gives rise to a different type of scattering. This two layer system represents optical properties of many human tissues with the first layer correlated with epithelium and second layer correlated with other tissue layers beneath epithelium. The upper layer is optically thin so that it does not allow multiple scattering. Small portions of incident linearly polarized light is backscattered by the particles in the upper layer. The rest of the signal penetrates to the second layer that is optically thick. Light propagating through the second layer is randomized by means of multiple scattering. This diffusive light, if not absorbed in the second layer, returns to the surface. Thus, emerging light has two contributions: one from light backscattered by the particles of the first layer, I_b, and the other being diffusely reflected from the second layer, I_d. I_b has high degree of linear polarization that is parallel to the polarization of the incident light: $I_{\parallel}^{b}>>I_{\perp}^{b}$. As a result of multiple scatterings in the second layer, diffusely reflected light is depolarized and $I_{\parallel}^{d}=I_{\perp}^{d}$. Therefore, the residual intensity of the emerging light $I_{\parallel}-I_{\perp}\approx I_{\parallel}^{b}-I_{\perp}^{b}$ is dominated by the contribution from the upper layer and is substantially free from both absorption and scattering from the tissue below.

Expressions (3)-(5) relate $I_{\parallel}-I_{\perp}$ to the scattering amplitudes S_1 and S_2. The amplitudes depend on the wavelength of the light being scattered $\lambda=\pi/k$, the scatter's size d and the ratio of its refractive index to that of the surrounding medium, relative refractive index n. Therefore, the spectrum of the residual intensity varies with the scatterer's size and relative refractive index. Thus, sizes and refractive indexes of the scatterers can be found by fitting the representation of the Mie theory using equations (3)-(5) to the residual intensity spectrum.

A system 10 that measures excised tissue samples *in vitro* is illustrated in Figure 1. This system 10 delivers collimated polarized light on tissue 12 and separates two orthogonal polarizations of back-scattered light. The difference of these two components provides information about light scattered in the epithelial layer only. Since linearly polarized light is depolarized faster than circularly

polarized light while passing through a random medium, linear polarization was used. The system provides light from a broad-band source 14 (250 W tungsten lamp, Model 66181, Oriel Instruments, Inc., Stratford, CT) is collimated and then refocused with a small solid angle onto the sample using a fiber 16, a lens 18 and an aperture 20. A broadband polarizer 22 linearly polarizes the beam, before it is delivered to the surface of a scattering medium through beamsplitter 24. The light beam strikes the surface of the sample with an angle ~15° relative to the normal in order to avoid specular reflectance. The diameter of the beam is 2mm. The reflected light is collected in a narrow cone (~0.015 radian) with apertures 26 and mirror 28 and two polarizations, parallel $I_{\|}$ and orthogonal $I_{\perp}$ to the initial polarization, are separated by a broadband polarizing beam splitter cube 28 which also acts as our analyzer (Melles Griot, Inc.). The output from this analyzer is delivered through lenses 30 and 200μm optical fibers 32, 34 (Ocean Optics, Inc., Dunedin, FL) into two channels of a multichannel spectroscope 36 (quadruple spectroscope, Model SQ200, Ocean Optics, Inc., Dunedin, FL). This enables the spectra of both components to be measured simultaneously in the range from 300 nm to 1200 or optionally in the range from 400 nm to 900 nm.

The beams are not perfectly collinear, and when they pass through the polarizer and analyzer cubes this gives rise to a small amount of distortion. Furthermore, the beamsplitter has different reflectivities for *s* and *p* polarizations. A diffusely reflective white surface was used as standard to correct for wavelength non-uniformity, and to calibrate the signals in the two channels. $I_{\perp}(\lambda)$ and $I_{\|}(\lambda)$ were each normalized to the corresponding background spectra, $I_{\perp}^{B}(\lambda)$ and $I_{\|}^{B}(\lambda)$ were each normalized to the corresponding background spectra, $I_{\|}^{B}(\lambda)$ and $I_{\perp}^{B}(\lambda)$ taken with the white diffusing surface. This removed spectral non-uniformities in the light source. Thus, the experiments actually measured the normalized residual intensity, ΔI:

$$\Delta I = \frac{I_{\parallel}}{I_{\parallel}^{B}} - \frac{I_{\perp}}{I_{\perp}^{B}}$$

(5)

Measurements on simple single- and two-layer systems were conducted to determine operational parameters. The single layer system included polystyrene beads of various sizes ranging from 0.5μm to 10μm (Polyscience, Inc.) embedded in de-ionized water, glycol, or glycerol. The thickness of these layers was varied so that the optical thickness τ ranged from 0.1 to 5 a photon propagating through a medium with τ=1, undergoes one scattering event on average). The beads of large sizes 4-10 μm were used to represent cell nuclei. Since the relative refractive index of the polystyrene beads in water is about 1.2 (absolute refractive index is about n=1.59) and is substantially higher than that of the cell nuclei relative to the cytoplasm which is in the range from 1.03 to 1.1, glycol (n_a=1.45) and glycerol (n_a=1.48) were used instead of water to decrease the relative refractive index of the beads and, therefore, better approximate biological conditions.

In the single layer measurements the component of the backscattered light with the same state of polarization as the incoming light (denoted by $I_{\parallel}$) was almost 100 times larger than the component with the polarization orthogonal to the polarization of the incoming light (denoted by $I_{\perp}$). This establishes that single scattering from large spheroidal particles preserves polarization.

In the measurements with two layer models the first layer consisted of polystyrene beads embedded in water, glycol, or glycerol and was prepared as in the single layer measurements. The second layer included a gel containing solution of $BaSO_4$ powder which provided scattering properties of the second layer and human blood. Hemoglobin content of the blood provided absorptive properties to the model. This physical model simulated epithelium and underlying tissues. Adjusting concentrations of the $BaSO_4$ powder and blood, the scattering and absorption properties, can be made similar to those of a biological tissue, since in the optical spectral region hemoglobin is known to be the major absorber.

Figures 2A and 2B shows spectra of the parallel $I_{\parallel}$ and orthogonal $I_{\perp}$ polarized components of the light reflected from a two layer system. In this measurement, the first layer contained beads embedded in glycol. The beads had an average diameter of 4.56 μm. Standard deviation of their sizes was 0.03 μm. Optical thickness of the first layer was $\tau \sim 0.8$. The second layer was optically thick and its scattering and absorptive properties were comparable to those of a biological tissue. The spectrum of $I_{\perp}$ is dominated by characteristic hemoglobin absorption bands. At the same time, characteristic spectral features of light scattered by 4.56 μm beads in the first layer, namely apparent ripple structure, and hemoglobin absorption in the second layer are seen in the spectrum of $I_{\parallel}$.

The residual spectrum ΔI is shown in Figure 3A. No hemoglobin absorption features are seen and the diffusive background coming from the second layer was completely removed. The ripple structure characteristic of scattering from spheres is evident. The comparison with Mie theory representation for scatterers with d = 4.56 μm , Δd=0.03μm and n=1.035 correspond with the μm shown in Figure 3B shows high degree of accuracy. The residual spectra obtained in measurements with other bead sizes (5.7μm, 8.9μm, and 9.5μm) embedded in any of the media used (water, glycol, and glycerol) had no measurable diffusive background component and agreed with Mie theory. Figure 3B shows the agreement between the theory and the measurements for 9.5 μm beads.

Similarly, the results of the measurements for 5.7 μm and 8.9 μm beads in glycerol and glycol are shown in Figures 3(C) and (D) respectively. Mie theory corresponds with the measured values in these cases as well. The high frequency ripple structure decreases as the relative refractive index gets smaller. The law frequency oscillations remain evident. Measurements showed that the instrument was able to detect signal from the bead solution of as low optical thickness as 0.05. Small disagreements seen in the spectrum can result from imperfect calibration of the instrument for the wavelength dependence of the optical elements used. The beams are not perfectly collinear and so there arises some imperfections in the polarized signals from the two channels when the beam passes through the polarizer

and the analyzer elements. Further, the beam splitter used has different reflectivities for the *s* and the *p* polarized beams. However, using just a white standard, signals in the two channels were corrected for any wavelength non-uniformity and further used for calibration of signals.

Measurements with cell monolayers were conducted and the results are described in connection with Figures 4-6. A layer of gel containing solution of $BaSO_4$ powder and human blood under the monolayers is used to represent underlying tissue. The concentrations of the $BaSO_4$ powder and blood, were adjusted to match optical properties of the biological tissue. Three types of cells were measured: normal intestinal cells, T84 cancer colonic cells and the fibroblasts. The measurements were similar to the measurements with beads. Nuclei of cells, however, had relative refractive indexes smaller then those of beads as well as larger size distributions which substantially eliminate the ripple structure. Fitting of the observed residual spectrum to Mie theory was performed. Three parameters in the fitting procedure were average size of the nuclei, standard deviation in size (a Gaussian size distribution was assumed), and relative refractive index.

For normal intestinal cells, the best fit was obtained using d=5.0μm,Δd=0.5μm, and n=1.045 (Figure 4). For the fibroblast cells, d-7.0 μm, Δd=1.0 μm and n=1.051 were obtained. For the T84 colon cancer cells the corresponding values were d=9.8 μm Δd=1.5 μm, and n=1.04 (Figure 5).

In order to check these results, the distribution of the average size of the cell nuclei was measured using light microscopy. The sizes and their standard deviations were in agreement with the parameters from Mie theory. A histogram showing the size distributions obtained for the normal T84 cells are shown in Figure 6. The accuracy of the average size is estimated to be 0.1 μm, and the accuracy in n as 0.001. Note the larger value of n obtained for cancerous cells, which is in agreement with the hyperchromaticity of cancer cell nuclei observed in conventional histopathology of stained tissue sections.

The backscattered signal can be described by Mie theory if the average size of the nuclei d, standard deviation in sizes Δd, and relative refractive index n are

varied. Note that in Mie theory, dependence on d and n does not always come as a $(n-1)d$ product. Thus, the residual spectra have enough information to extract d and n simultaneously.

The size distributions for monolayers were compared to light microscopy and were in a good agreement for all three lines of cells. The accuracy of size and standard deviation extraction was approximately 0.1 μm which makes the method useful in differentiating nuclei of different cell types, including cancerous and non-cancerous cells of the same organ.

Ability to detect cell nuclear enlargement and changes in refractive index of the nucleus (which can be related to the amount of DNA and protein in the nucleus) has valuable applications in clinical medicine.

The method of tissue diagnosis can be implemented either in a diagnostic device in which light can be delivered to points on the surface of the tissue, and collected and analyzed at each of those points on the surface of the tissue, and collected and analyzed at each of those points. In an *in vivo* system optical fibers are used to deliver and collect light. The fiber probe can be inserted in the endoscope biopsy channel or any similar device (depending on the type of the procedure and organ under study). Polarizer and analyzer can be placed at the tip of the probe in front of the delivery and collection fibers. Such an instrument can be used during routine endoscopic procedures to detect precancerous changes *in-vivo* in real time.

Such a probe system 40 is shown generally in Figure 7. This system 40 includes a broadband light source 42 that is optically coupled to a delivery fiber 44 extending through probe 50. As schematically shown in Figure 7, the probe 50 can be inserted through a channel in an endoscope 48, however the probe 50 can be constructed to be used separately. In a preferred embodiment described hereinafter, the light from source is directed through a polarizer at the distal end of probe 50. However, in another embodiment using polarization preserving optical fibers, a polarizer 26 can be used at the proximal end of probe fiber 44 to direct polarized light 46 through the fiber. Similarly, the proximal ends of collection fibers 65, 66 can employ polarizing elements 65, 66 respectively to transmit selected polarization

components into the multichannel fiber spectrometer 54. The data can then be processed by computer 56, stored in computer 56, stored in computer memory and displayed on display 60 as needed.

The probe system can include a fiber optic probe having a distal end incorporating polarizers as seen in Figure 8A and 8B.

Figures 8A and 8B show the distal end of a probe 100 for the use of polarized light for in vivo diagnosis. Figure 8A shows a fiber optic device that is divided into three sections, the inner delivery fiber and two sets of collection fibers 150 and 152 that collect different polarization components. The cross-section of Figure 8B shows fibers 156 delivering light onto the tissue 140. They have to pass through a polarizer 120 which is also seen in the cross-section view of Figure 8B. The polarizing element is divided into at least two parts or elements 122, 126. Optical fibers 152 are arranged to collect the back reflected light from the tissue surface.

The backscattered light has two polarization components, corresponding to the parallel and the perpendicular components to the incident light. The two are differentiated by two different birefringent analyzers shown by two sectioned ring elements 122, 126. A first element 122 allows the parallel component to pass through while the second element 126 allows perpendicular component. A portion of element 122 polarizes light exiting fiber 156. As the fibers have low numerical apertures to collect light over very small angles, it is necessary to extend the distance 136 between the fiber ends and the aperture surface 142 opening to the tissue surface 140. It can be as long as 5mm. To avoid spurious internal reflections a glass block 130 is shown having refractive index n_2 lower than that of the shield 132 with refractive index n_1. The shield 132 can be coated with an absorbing element so that light hitting the boundaries is refracted out and then absorbed by the absorbing coating on the outer wall of the shield 132. The glass element 130 is beveled to avoid specular reflections from the tissue surface as it is described to increase the relative signal strength of the back-scattering. The light having the two orthogonal

polarizations is separated and coupled to two spectrometer channels for detection and analysis.

Another preferred embodiment of a fiber optic probe 160 is illustrated in Figures 9A-9C. In this embodiment, delivery 156 and collection 162 fibers are housed in flexible tube 164 that is attached to a distal annular housing 166. Housing 166 includes a fiber retainer 106 and a polarizer 168 which can be a birefringent crystal such as calcite, quartz or sapphire. Delivery fiber 156 delivers light from source 42 to polarizer 168 which delivers ordinary ray 170 through aperture 175 and window 178. Light returning through aperture 175 has ordinary 170 and extraordinary 172 components. The perpendicular component is collected by fibers 162 and the parallel component is collected by fibers 161. The delivery fiber 156 is positioned along the optical axis 176 of the crystal 168. Fibers 161, 156 are aligned along the aperture 175 of absorbing plate 178.

While this invention has been particularly shown and described with references to preferred embodiments thereof, it will be understood by those skilled in the art that various changes in form and details may be made therein without departing from the spirit and scope of the invention as defined by the appended claims.

CLAIMS

What is claimed is:

1. A method of analyzing polarized light comprising:

detecting polarized light returning from a region of interest; and

determining a characteristic of the region of interest by analyzing the detected polarized light.

2. The method of Claim 1 further comprising determining a size of tissue cells within the region of interest.

3. The method of Claim 1 further comprising removing a nonpolarized component of the light returning from tissue.

4. The method of Claim 1 further comprising providing a fiber optic probe and collecting polarized light from the tissue with the probe.

5. The method of Claim 1 further comprising detecting the polarized backscattered light and forming a spectrum with the detected light, the spectrum including wavelengths in the range of 300 nm to 1200 nm.

6. The method of Claim 1 further comprising determining a fracture index of the region of interest with the detected polarized light

7. The method of Claim 1 further comprising detecting light from a tissue sample.

8. The method of Claim 7 further comprising providing a broadband light source and a filter wheel and delivering polarized light onto the tissue sample.

9. The method of Claim 1 further comprising separating polarization components of light returning from the region of interest and analyzing the two components to remove non-polarized backscattered light from the detected light.

10. A fiber optic probe for measuring a layer of tissue comprising:

a fiber optic cable optically coupled to a light source, the fiber optic cable delivering polarized light onto the tissue; and

a detector system that detects the polarization components of light received from the tissue.

11. The probe of Claim 10 further comprising a polarizer that polarizes light from the light source, the polarizer positioned at a distal end of the fiber optic cable.

12. The probe of Claim 10 further comprising an analyzer that separates polarization components returning from tissue through the fiber optic cable.

13. The probe of Claim 10 further comprising an endoscope having a channel through which the probe is inserted.

14. The probe of Claim 12 wherein the analyzer comprises a polarizing beam splitter.

15. The probe of Claim 12 wherein the analyzer is positioned at a distal end of the fiber optic cable.

16. The probe of Claim 10 further comprising a plurality of polarization filters at the distal end of the probe.

17. The probe of Claim 10 wherein the light source comprises a broadband light source and a filter wheel.

18. The probe of Claim 10 further comprising a spectrometer optically coupled to the fiber optic probe.

19. The probe of Claim 10 further comprising an electronic memory that stores spectra, the spectra including wavelengths in the range of 300nm to 1200nm.

20. The probe of Claim 10 further comprising a computer that analyzes detected spectra to determine whether a surface layer of tissue is normal or epithelial dysplasia.

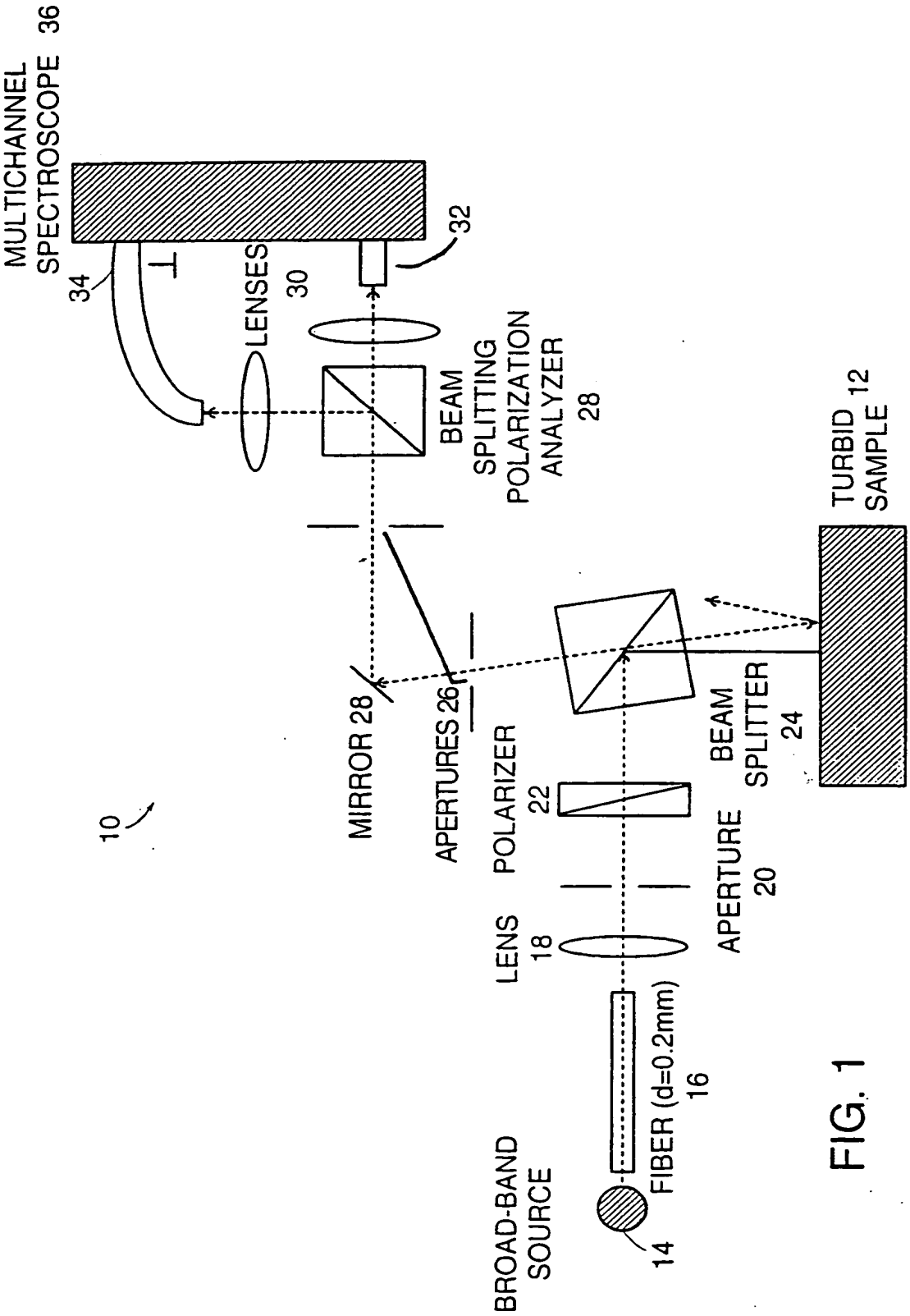
MULTICHANNEL SPECTROSCOPE 36
34
LENSES 30
32
BEAM SPLITTING POLARIZATION ANALYZER 28
TURBID SAMPLE 12
MIRROR 28
APERTURES 26
POLARIZER 22
BEAM SPLITTER 24
10
LENS 18
APERTURE 20
BROAD-BAND SOURCE
14
FIBER (d=0.2mm) 16

FIG. 1

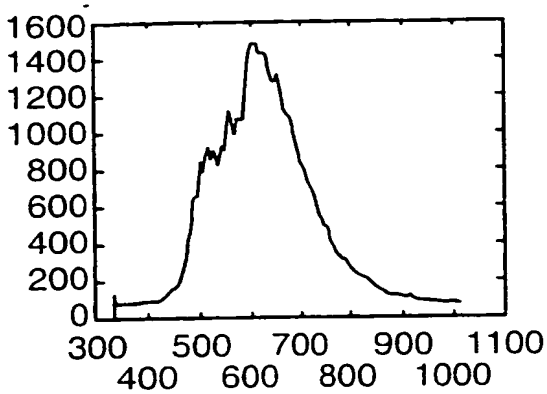

FIG. 2A

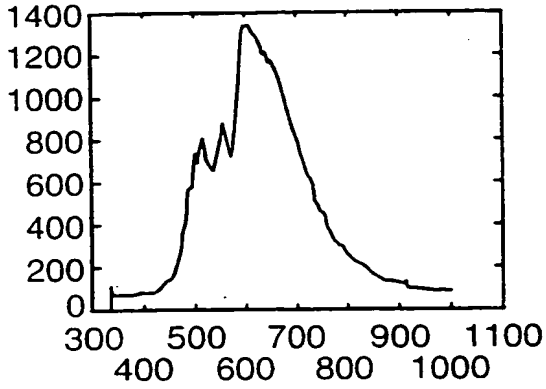

FIG. 2B

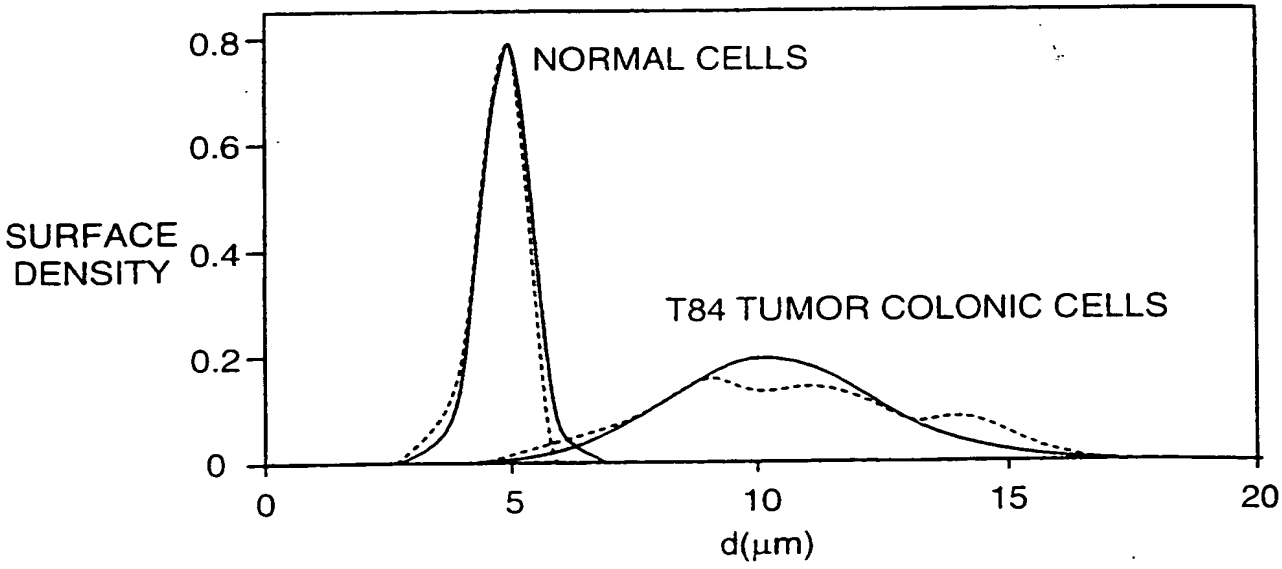

FIG. 6

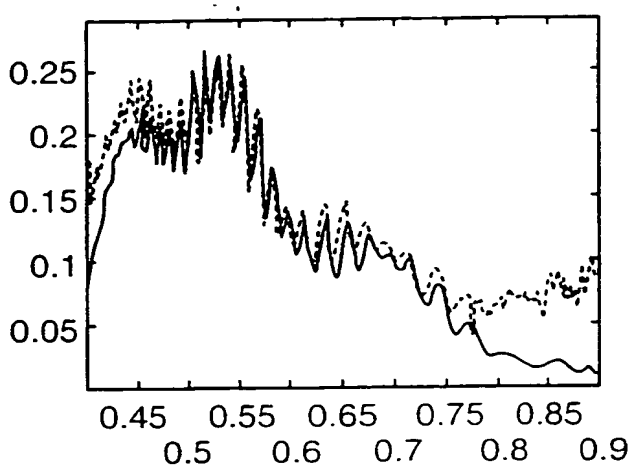

FIG. 3A

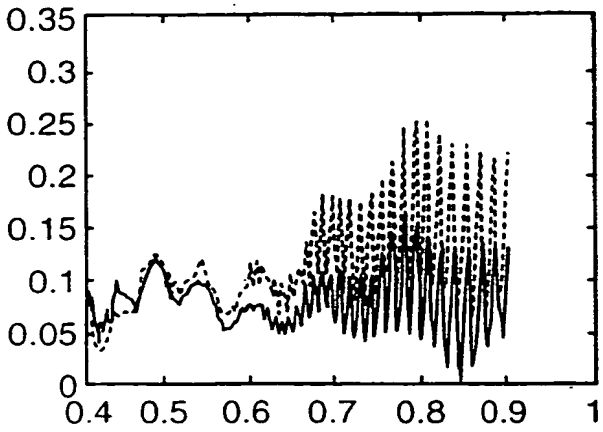

FIG. 3B

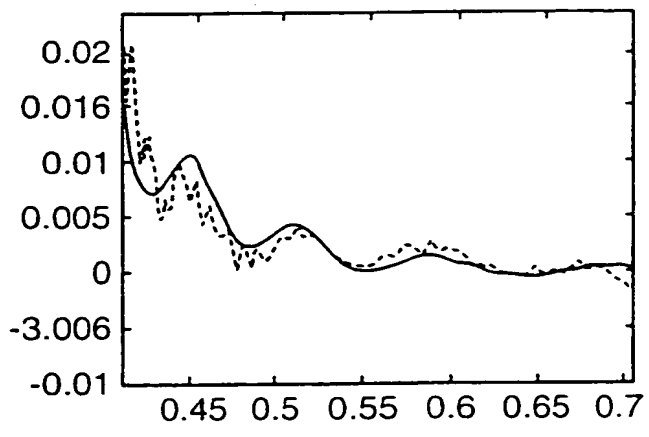

FIG. 3C

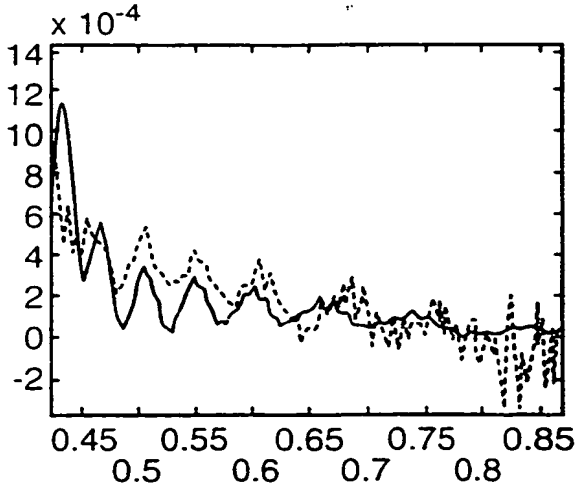

FIG. 3D

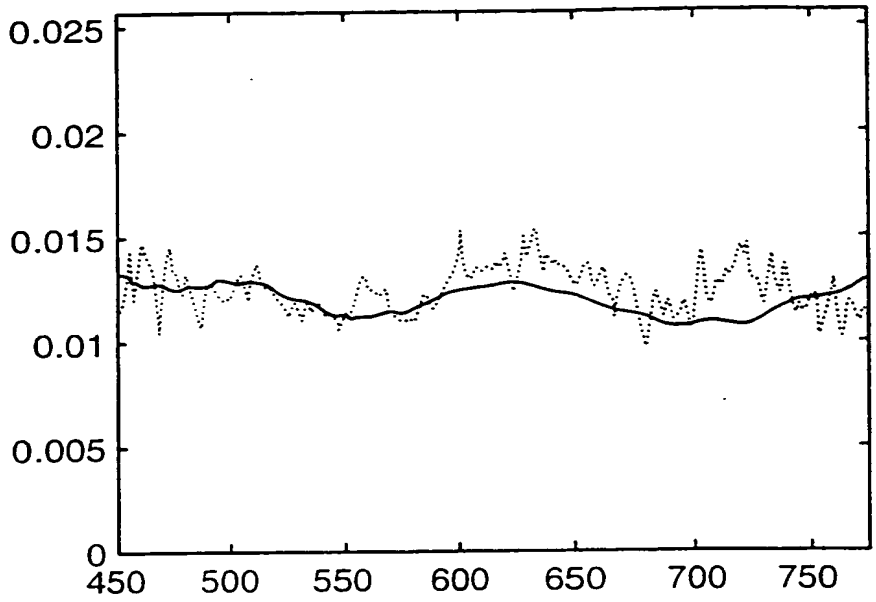
0.025
0.02
0.015
0.01
0.005
0
450
500
550
600
650
700
750

FIG. 4

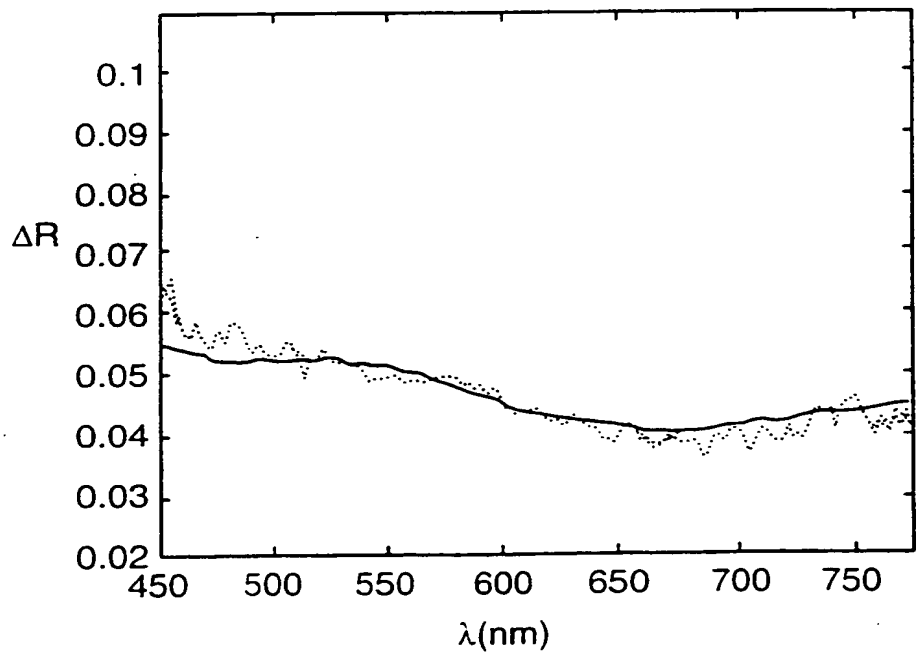
0.1
0.09
0.08
0.07
0.06
0.05
0.04
0.03
0.02
ΔR
450
500
550
600
650
700
750
λ(nm)

FIG. 5

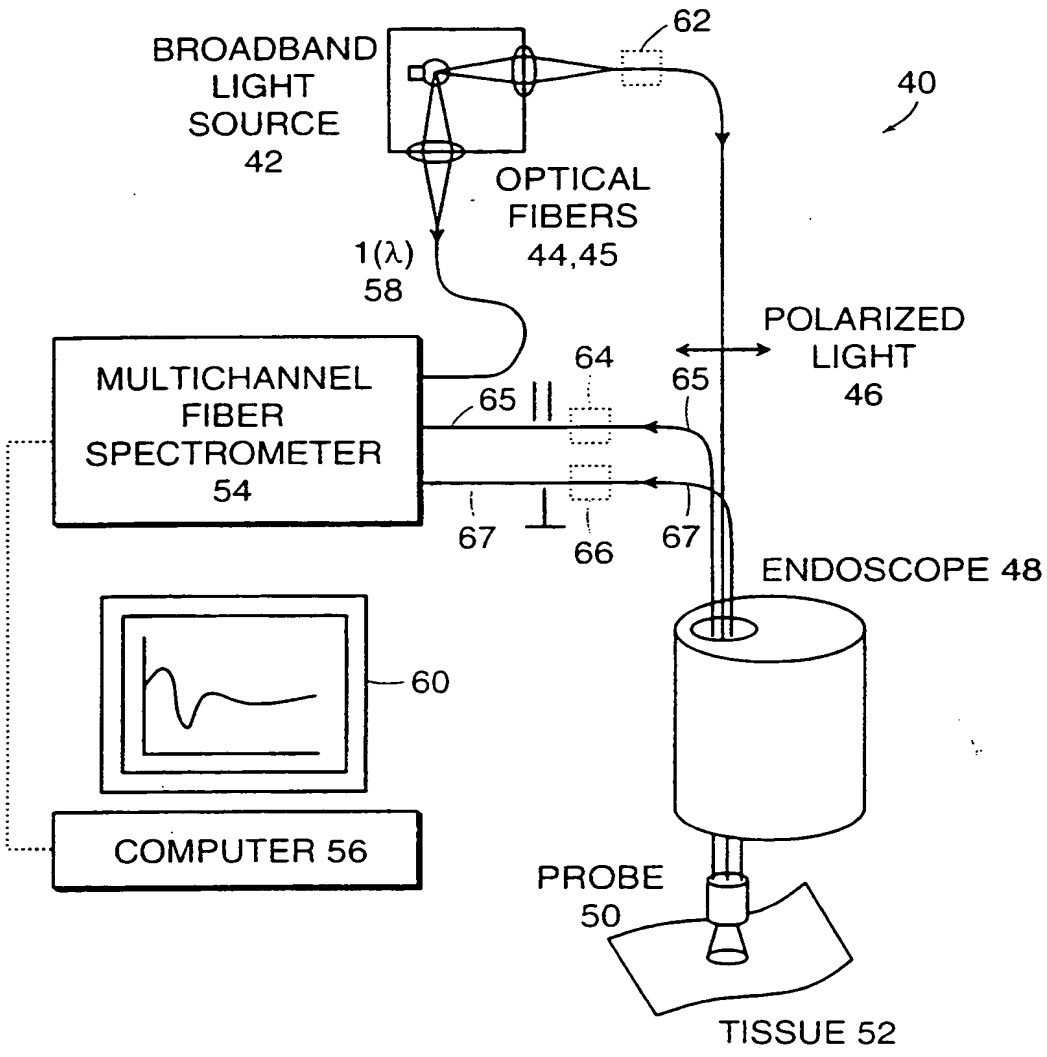

FIG. 7

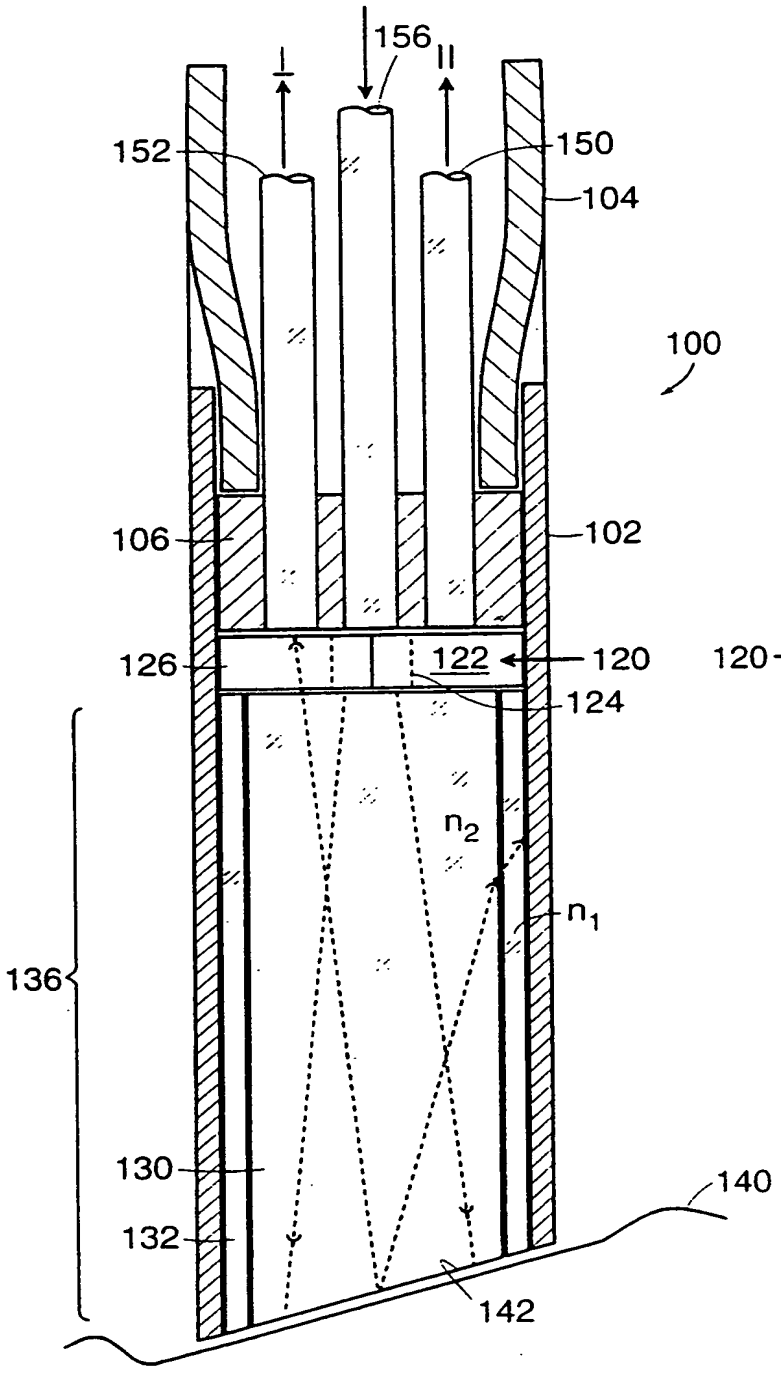
156
152
150
104
100
106
102
126
122
120
124
n_2
n_1
136
130
140
132
142

FIG. 8A

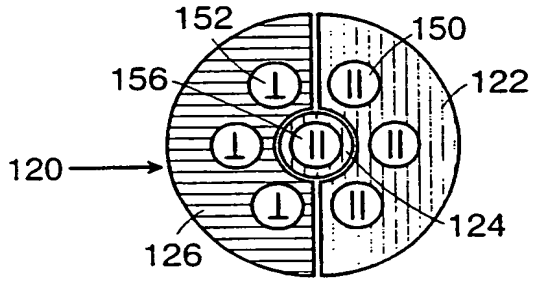
152
150
156
122
120
124
126

FIG. 8B

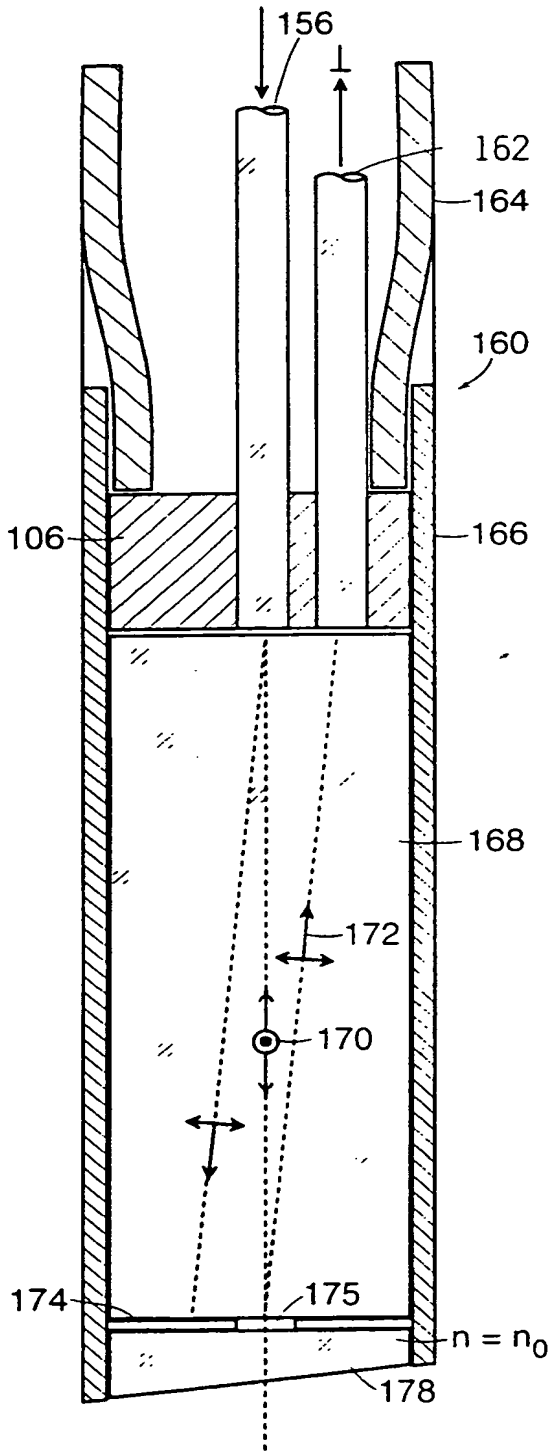

FIG. 9A

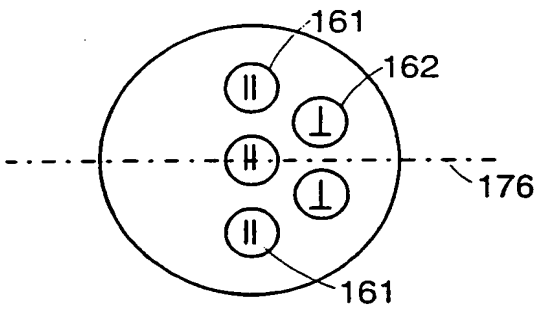

FIG. 9B

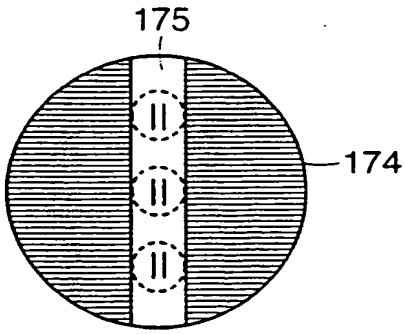

FIG. 9C

INTERNATIONAL SEARCH REPORT

.ernational Application No
PCT/US 00/01967

A. CLASSIFICATION OF SUBJECT MATTER
IPC 7 A61B5/00

According to International Patent Classification (IPC) or to both national classification and IPC

B. FIELDS SEARCHED

Minimum documentation searched (classification system followed by classification symbols)
IPC 7 A61B

Documentation searched other than minimum documentation to the extent that such documents are included in the fields searched

Electronic data base consulted during the international search (name of data base and, where practical, search terms used)

C. DOCUMENTS CONSIDERED TO BE RELEVANT

Category °	Citation of document, with indication, where appropriate, of the relevant passages	Relevant to claim No.
X	US 5 290 275 A (COTHREN JR ROBERT M ET AL) 1 March 1994 (1994-03-01) figures 4,13C,19,20	1-20
A	US 5 333 052 A (FINAROV MOSHE) 26 July 1994 (1994-07-26) figure 1	1-20
A	US 5 813 987 A (DEBARYSHE GREGORY ET AL) 29 September 1998 (1998-09-29) figure 2	1-20
A	US 5 280 788 A (JANES G SARGENT ET AL) 25 January 1994 (1994-01-25) figure 14	1-20

-/--

[X] Further documents are listed in the continuation of box C.

[X] Patent family members are listed in annex.

° Special categories of cited documents :

"A" document defining the general state of the art which is not considered to be of particular relevance

"E" earlier document but published on or after the international filing date

"L" document which may throw doubts on priority claim(s) or which is cited to establish the publication date of another citation or other special reason (as specified)

"O" document referring to an oral disclosure, use, exhibition or other means

"P" document published prior to the international filing date but later than the priority date claimed

"T" later document published after the international filing date or priority date and not in conflict with the application but cited to understand the principle or theory underlying the invention

"X" document of particular relevance; the claimed invention cannot be considered novel or cannot be considered to involve an inventive step when the document is taken alone

"Y" document of particular relevance; the claimed invention cannot be considered to involve an inventive step when the document is combined with one or more other such documents, such combination being obvious to a person skilled in the art.

"&" document member of the same patent family

Date of the actual completion of the international search	Date of mailing of the international search report
15 June 2000	26/06/2000

Name and mailing address of the ISA	Authorized officer
European Patent Office, P.B. 5818 Patentlaan 2 NL - 2280 HV Rijswijk Tel. (+31-70) 340-2040, Tx. 31 651 epo nl, Fax: (+31-70) 340-3016	Mason, W

1

Form PCT/ISA/210 (second sheet) (July 1992)

INTERNATIONAL SEARCH REPORT

ternational Application No
PCT/US 00/01967

C.(Continuation) DOCUMENTS CONSIDERED TO BE RELEVANT

Category ³	Citation of document, with indication, where appropriate, of the relevant passages	Relevant to claim No.
A	US 5 014 709 A (BJELKHAGEN HANS ET AL) 14 May 1991 (1991-05-14) figure 1A	1-20
A	US 4 768 513 A (SUZUKI SUSUMU) 6 September 1988 (1988-09-06) figure 1	1-20
A	WO 98 38907 A (MASSACHUSETTS INST TECHNOLOGY) 11 September 1998 (1998-09-11) page 14	1-20

Form PCT/ISA/210 (continuation of second sheet) (July 1992)

INTERNATIONAL SEARCH REPORT

Information on patent family members

ernational Application No
PCT/US 00/01967

Patent document cited in search report	Publication date	Patent family member(s)	Publication date
US 5290275 A	01-03-1994	US 4913142 A	03-04-1990
		US 5034010 A	23-07-1991
		US 5304173 A	19-04-1994
		US 5106387 A	21-04-1992
		US 5199431 A	06-04-1993
		US 5104392 A	14-04-1992
		US 5693043 A	02-12-1997
		US 5318024 A	07-06-1994
		US 5496305 A	05-03-1996
		AT 111711 T	15-10-1994
		AT 167792 T	15-07-1998
		CA 1279901 A	05-02-1991
		CA 1339056 A	29-07-1997
		CA 1317641 A	11-05-1993
		CA 1329655 A	17-05-1994
		DE 3650071 D	27-10-1994
		DE 3650071 T	01-06-1995
		DE 3650688 D	06-08-1998
		DE 3650688 T	25-03-1999
		DK 130586 A	23-09-1986
		EP 0195375 A	24-09-1986
		EP 0590268 A	06-04-1994
		FI 861209 A	23-09-1986
		JP 2589674 B	12-03-1997
		JP 61257638 A	15-11-1986
		JP 2739933 B	15-04-1998
		JP 9117407 A	06-05-1997
		NO 861136 A	16-01-1987
US 5333052 A	26-07-1994	IL 96483 A	31-07-1995
		EP 0563221 A	06-10-1993
		JP 2702281 B	21-01-1998
		JP 6504843 T	02-06-1994
		WO 9209880 A	11-06-1992
US 5813987 A	29-09-1998	AU 6645796 A	26-02-1997
		CA 2228308 A	13-02-1997
		EP 0842412 A	20-05-1998
		JP 11510254 T	07-09-1999
		WO 9705473 A	13-02-1997
US 5280788 A	25-01-1994	EP 0575472 A	29-12-1993
		WO 9214399 A	03-09-1992
US 5014709 A	14-05-1991	NONE	
US 4768513 A	06-09-1988	JP 62247232 A	28-10-1987
WO 9838907 A	11-09-1998	EP 0971626 A	19-01-2000